Master's thesis

NTNU
Norwegian University of Science and Technology
Faculty of Engineering
Department of Energy and Process Engineering

Kristen Bernhard Holtaas Sandaas

Implementing Renewable Electrification: Forecasting Requirements for Global LIB ESS Deployment

Master's thesis in Mechanical Engineering
Supervisor: Jacob Joseph Lamb
Co-supervisor: Lorenzo Usai
June 2022

NTNU
Norwegian University of Science and Technology

Kristen Bernhard Holtaas Sandaas

Implementing Renewable Electrification: Forecasting Requirements for Global LIB ESS Deployment

Master's thesis in Mechanical Engineering
Supervisor: Jacob Joseph Lamb
Co-supervisor: Lorenzo Usai
June 2022

Norwegian University of Science and Technology
Faculty of Engineering
Department of Energy and Process Engineering

NTNU
Norwegian University of
Science and Technology

Preface

In their final semester at NTNU, students in the 5 year program of Mechanical Engineering will submit their master's thesis. The author wants to express gratitude to supervisor Associate Professor Jacob Joseph Lamb, as well as PhD Candidate Lorenzo Usai for their guidance and support during the writing process.

Abstract

In order to lower greenhouse gas emissions from the global electricity sector and contribute less to climate change, large amounts of renewable energy is predicted to be installed in the coming decades. According to scenarios by the International Energy Agency, most of this increase is going to be covered by wind and solar power, which are non-controllable resources and increases the requirement for grid energy storage. In this thesis, the energy capacity, material requirements and greenhouse gas emissions of lithium ion battery energy storage for three different IEA scenarios until 2050 were estimated. A spreadsheet model was created in order to analyse the requirements. A close to exponential relationship between energy storage requirements and variable renewable energy penetration was observed. For the most ambitious scenario, the material requirements would be close to the current reserves of several materials, while this would not be the case for the least ambitious scenario. Substantial greenhouse gas emissions from production of the batteries was found, but with a lowering intensity over time for the two least ambitious scenarios, as a cleaner power mix makes battery manufacturing less climate intensive.

Sammendrag

For å redusere klimagassutslippene fra den globale elektrisitetssektoren og bidra mindre til klimaendringer, er det spådd at store mengder fornybar energi vil bli installert i de kommende tiårene. I følge scenarier fra Det Internasjonale Energibyrået vil det meste av denne økningen dekkes av vind- og solkraft, som er ikke-regulerbare ressurser som øker behovet for energilagring. I denne oppgaven ble energikapasitet, materialbehov og klimagassutslipp av litiumionbatteri-energilagring for tre forskjellige IEA-scenarier frem til 2050 estimert. En regnearkmodell ble laget for å analysere kravene. En nær eksponentiell sammenheng mellom krav til energilagringskapasitet og variabel fornybar energiandel i energimiksen ble observert. For det mest ambisiøse scenariet vil materialbehovet ligge nær dagens reserver av flere materialer, mens dette ikke vil være tilfellet for det minst ambisiøse scenariet. Det ble funnet betydelige klimagassutslipp fra produksjon av batteriene, men med en avtagende intensitet over tid for de to minst ambisiøse scenariene, da en renere kraftmiks gjør batteriproduksjonen mindre klimafiendtlig.

Table of Contents

Acronyms

LIB = Lithium Ion Battery

VRE = Variable Renewable Energy

BEV = Battery Electric Vehicle

PHEV = Plug in Hybrid Electric Vehicle

GHG = Greenhouse Gas

ESS = Energy Storage System

BES System, BESS = Battery Energy Storage System

IEA = International Energy Agency

NZE = Net Zero by 2050 Scenario

APS = Announced Pledges Scenario

STEPS = Stated Policies Scenario

LFP = Lithium Iron Phosphate

NMC = Nickel Manganese Cobalt

LMO = Lithium Manganese Oxide

LCO = Lithium Cobalt Oxide

PV = Photovoltaic

DRC = Democratic Republic of the Congo

BatPaC = Battery Manufacturing Cost Estimation

ANL = Argonne National Laboratory

LLI = Loss of Lithium Inventory

LAM = Loss of Active Material

SEI = Solid Electrolyte Interphase

CEI = Cathode Electrolyte Interphase

SOC = State of Charge

DOD = Depth of Discharge

EFC = Equivalent Full Cycles

TMS = Thermal Management System

LCA = Life Cycle Assessment

ARC = Accelerated Rate Calimetry

List of Figures

List of Tables

1 Introduction

In 1882, Thomas Edison opened the US' first commercial electric power plant in Pearl Street, New York. Ever since, the world has been reliant on electric power to light up homes, streets and power the global industry. Edison's plant in New York worked by burning coal in a boiler, generating steam to power large steam engines, which powered electrical generators[42]. 140 years later, in 2022, 36.7 % of global electricity is still generated from burning the same fuel; coal. Additionally, gas contributes with another 23.5 %. In total, the majority of the world's electricity is generated from the combustion of fossil fuels[37]. Fossil fuel production and combustion releases the greenhouse gas CO2, which is largely responsible for causing global climate change, which can have catastrophic future effects on human society and Earth's living conditions and is already causing large-scale destruction all over the world[55]. Because of this, 196 countries have signed the Paris Climate Accords, which is a legally binding treaty which aims to limit the global warming to 2, or most preferably 1.5 degrees C compared to pre-industrial levels. To achieve this, all nations would have to rapidly transition their economy away from fossil fuels.

According to the International Energy Agency (IEA), the announced pledges by governments today, even if fulfilled, fall short of making humanity reach the 1.5 degree target. The agency has therefore developed the Net Zero By 2050 (NZE) scenario, which is a study on how to transition the global energy system towards zero net GHG emissions by 2050. The electricity sector is the largest single source of energy-related CO2 emissions, being responsible for 36 % of the emissions from the energy sector[15]. Decarbonising global electricity production is therefore a high priority in order to lower the energy-related emissions. In the NZE report, widespread adoption of renewable energy is the most contributing factor to lowering GHG emissions. Additionally, the NZE scenario predicts a high degree of electrification. In 2050, NZE predicts that 60 % of new car sales are BEVs, and that low and medium heating, as well as industry, will electrify. This will more than double electricity demands. The main drivers for zero-carbon electricity is predicted to be wind turbines and solar PV, with 2050 generation of these energy sources being 35 and 33 %, respectively. Consequently, 68 %, or the majority of electricity generation, is going to be covered by wind and solar PV in 2050[15].

Solar PV and wind turbines are examples of variable renewable energy (VRE). Unlike most current power plants, this is a type of renewable energy which has a non-controllable power output. In order to ensure grid stability and flexibility, NZE calls for ways to compensate for the growing unpredictability of power generation: More demand-side management, invest in flexible renewable energy like hydroelectric power plants and bioenergy, and expand battery storage. At the same time as VRE sources penetrate the power grid in increasing rate and the demand for energy storage rises, the world is also witnessing the rapid increase in availability of affordable and efficient rechargeable batteries with high specific energy capacity. This technology is mainly centred on the lithium ion battery (LIB), which was first patented in 1985 by Goodenough[19].

Lithium ion batteries have largely replaced the earlier nickel metal-hydride and nickel-cadmium batteries in electronics and automotive applications, and are rapidly entering the energy storage market. One of the most favourable aspects of the LIB is the relatively high specific/volumetric energy density of 100-265 Wh/kg or 250-670 Wh/L[46], which makes them useful for transport electrification. The first LIBs were based on the Lithium Cobalt Oxide cathode chemistry (LCO). Major research has already been conducted on improving various aspects of the LIB, and as such a multitude of different variations and chemistry types have been developed, which have led to a

dramatic decrease in cost and increase in energy density and lifetime.

In this thesis, NZE will be used as a base to forecast the requirements of a future where VRE sources become the majority of global electricity production. In this analysis, four requirements of the global lithium ion battery storage system (LIB ESS) towards 2050 will be examined:

A. The required global installed LIB ESS capacity to satisfy the NZE scenario's VRE penetration.

B. The inflow and outflow of LIB ESS to sustain the required installed capacity.

C. The raw material required to sustain the estimated inflow and outflow values.

D. The greenhouse gas emissions of manufacturing the required amount of LIB ESS systems.

While the IEA's NZE scenario was the main motivation for performing this analysis, two other scenarios will also be analysed, to provide needed context and more conservative outlooks than the NZE. These will be the Announced Pledges Scenario (APS) and Stated Policies Scenario (STEPS). Unlike NZE, these two scenarios were not designed to aim for a particular outcome, but are rather based on existing policies. The Announced Pledges Scenario forecasts a scenario where the currently announced GHG emission pledges of governments are fulfilled. In this less ambitious scenario, net zero GHG emissions are not necessarily implemented, but are assumed by some countries to be counteracted by absorption of forests or land use. The Stated Policies Scenario provides a more conservative outlook than NZE and APS. In this scenario, the current pledges by governments are not taken for granted, and rather takes an approach that explores the direction the global energy system will go without any major push by policy makers[7][73].

In this thesis, the four previously discussed requirements for the 2021-2050 global developments in LIB ESS will be analysed for the NZE, APS and STEPS scenarios. The results of each scenario will then be compared. Challenges, opportunities and other findings will then be identified to bring the scope of this analysis into a wider context, to connect it with the rest of the energy industry and LIB sector.

2 Theory

2.1 Introduction to Grid Energy Storage

The focus of this thesis is going to be the topic of grid energy storage, which can also be referred to as energy storage systems (ESS). These two terms will be used interchangeably. In this section, the functionality of the electric grid will be briefly explained, and the different challenges of the future electricity mix will be described. Lastly, an introduction to grid energy storage will be given, as well as some examples of ESS in use today.

2.1.1 The Electric Grid: Supply and Demand on a Massive Scale

In order to make electrical power practical and affordable for home, industrial, and commercial applications, the electrical energy needs to be transported from where it's produced to where it's needed. This is achieved through an electrical grid, where the process of power transmission can be typically divided into three distinct steps: Production, transmission and distribution[29]. As this thesis will be concentrated on energy storage systems, this section will be a brief introduction to the basic functionality of power grids and why efficient energy storage is necessary for a future where renewable energy is more dominant than it is today.

The first step in any electrical grid is production, where one form of energy (for example chemical, mechanical, nuclear energy) is converted into electrical energy in a facility usually referred to as a power plant. After the electricity is produced, it's converted to high voltage (normally in the range of hundreds of kilovolts) in a step-up transformer, and transmitted closer to the geographic location where the power is needed. By using alternating current at a high voltage, power loss for long distances is minimised. The transmission itself is achieved by using high voltage lines connected from the production locations, which are usually located remotely, to the distribution networks, which are usually closer to the final use location. The final step is the distribution process. In distribution, the high voltage power from the transmission network is stepped down to a lower voltage and distributed to the customers through transformers stepping down the voltage to safer and more manageable levels, which in Norway and Europe is usually 230 Volts[30][81].

The first step in any power grid is the electricity generation itself. Traditionally, this has been achieved by generators connected to rotating shafts, which convert mechanical power into electric power. The main distinction between different types of power plants is usually the means of generating the mechanical power to turn the generator shafts. One of the first methods for generating shaft power is still used today, in the form of hydroelectric power plants, which use the potential energy of water to generate vast amounts of electricity[51]. Where the geography couldn't allow hydro power to be utilised, thermal power plants have been used, also known as conventional power plants[66]. Thermal power plants convert the chemical energy of fuels into thermal energy, where fossil fuels like coal or oil are burned, converting the thermal energy into mechanical energy through the use of heat engines. Most commonly, thermal power plants use the Rankine cycle, but other cycles like the Brayton or Diesel cycle are also used, depending on the fuel and operating regime. Because heat engines like the Rankine cycle are not dependent on a specific source of heat, the heat can also be sourced by other means, like nuclear fission, geothermal heat or concentrated solar power[52].

Figure 1: The NZE scenario envisions a large shift towards variable renewable energy. (Photo by author)

The vast majority of electricity generated at power plants is consumed almost the instant its generated. It is therefore critical that the electric power generation is controllable, so that the supply always follows the demand. Conventional power plants are therefore designed to respond to the load changes of the grid. Some types of conventional power plants respond quicker than others, and are typically used in different ways according to the current demand[5]. Additionally, electricity demand and production usually follows relatively predictable patterns, referred to as different loads. These loads vary depending on time of day and other factors, as different customers demand different amounts of power at a given time of day. Power plants can be grouped into different types based on their operating regime[5][8]:

Base Load. The base load is the constant demand of electricity by society, often covered by power plants which can not quickly change their output and are more efficient at a constant load. Nuclear plants are an example of this[8].

Medium Load. This is the load which is still relatively constant, but can fluctuate based on time of day and other factors. Therefore, power plants operating in this regime need to be able to change their output, but not as quickly as other types.

Peak Load. Peak load is covered by power plants that can respond quickly to changes in demand, as changes in peak demands often occur rapidly in comparison to the aforementioned examples. For this situation, natural gas power plants are normally used. Additionally, high peak demands may also occur, which is covered by specialised peaker plants, normally using open cycle gas turbines, which have an even faster response[5].

2.1.2 The Challenges of Going Green

Traditionally, electricity production and demand closely follows each other. Unlike other forms of commodities, electrical energy has traditionally been difficult to store efficiently and cheaply, so the simplest solution has been to just increase and decrease production when needed. However, in order to respond to the looming threat of anthropogenic climate change, which is partially caused by humanity's combustion of fossil fuels for electricity generation, large investments are predicted to be put into building out more renewable energy, with the goal of ending human dependence on fossil energy[20][15]. However, the introduction of more renewable energy poses large, fundamental challenges to the global power grid.

When discussing renewable energy, it is important to show distinction between so-called controllable renewable energy and variable renewable energy (VRE). Controllable renewable energy are energy sources of renewable origin that can be utilised according to demand, in a similar way to conventional power plants. Examples of these are hydroelectric power plants and biomass. Variable renewable energy is renewable sources of energy that produce electricity without a consideration to current demand[11]. This is mainly a feature of wind turbines and solar power (photovoltaic, or PV), of which both have seen large increases in adoption during recent years and decades[15]. These sources have some challenges that are unique compared to conventional power plants and controllable renewable energy.

When using wind or solar power, the variability of production means that energy load and supply is disconnected from each other. For solar plants, the supply mainly depends on time of day, season and cloud cover. The theoretical power output of solar photovoltaic panels is generally quite predictable, as the position of the Sun at a given time is a well-known scientific phenomenon. On the other hand, cloud cover is less predictable, and can greatly affect the power output of individual PV panels, although spreading the PV plants over a wide geographical area will tend to smooth out the power production[21][11]. Wind power is subject to less predictability, but will tend to correspond with weather patterns that follows daily and seasonal trends. Wind turbines generally experience slower changes in output compared to solar, and can also produce power at nighttime[11]. This is currently impossible with solar PV plants unless they are located above the Arctic Circle in the summer.

This variability means that other parts of the grid needs to be able to quickly compensate for the VRE sources' increasing or decreasing share of production. Some types of conventional power plants have this ability by design, like gas turbine peaking plants[5]. Power sources traditionally more suited to base or medium load will be less suited for rapid changes in output. For such situations, a power plant may need to run at part-load, or needing to start or stop more often (cycling). This can lead to damage and lower efficiency for conventional power plants, especially those designed to be base-load types [11].

Another challenge is the topic of grid inertia. In conventional and hydroelectric power plants, the generating units typically consists of large, heavy turbines connected to synchronous generators. The rotational velocity of the spinning turbine and generator is maintained at a constant speed which corresponds to the grid frequency. Due to the large moment of inertia of this spinning system, the frequency of the grid is able to keep relatively constant during short-term changes in load, with the mass of the generators performing kinetic energy storage, in essence acting like flywheels[25]. VRE sources, like wind turbines and photovoltaic panels, do not have this inherent

Figure 2: Hydroelectric power is renewable and can easily be regulated. (Photo by author)

trait to the same degree, as they typically supply power to the grid through power electronics, not generators running at grid frequency.

There are several methods available to resolve the previously mentioned issues, many of which are used at the same time. The variability problem can be alleviated by utilising more advanced forecasting, by being able to more accurately predict electricity demand over the course of the day. It can also be used to determine the availability of wind or sunlight, allowing operators to more accurately assess the future availability of VRE sources[11].

Additionally, the method of demand response (DR) can be used, which aims to control electricity demand rather than supply. DR attempts to control demand during certain periods to better match the currently available supply. DR can be achieved by several different methods, some of which are economic, others are technical[11]. A common method is to use variable electricity pricing to insentivise the customers to use less power in certain periods of low supply, or otherwise use more in periods of high supply. This can be achieved with off peak pricing (for instance, having a lower electricity price at night) or by using smart meters, which dynamically meter according to current electricity cost, allowing the customer to turn off power-intensive equipment during periods of high cost. The same result can also be achieved technologically, with power-intensive appliances using demand response switches to be used in periods of high supply, and vice versa.

Another option, which will be the main focus of this thesis, is using grid energy storage systems (ESS). ESS allows the storage of intermittent VRE energy to be reclaimed for a later time, which resolves the variability issue of VRE sources. Different ESS work by different principles which will be explored in the next sections. The common trait of any grid energy storage system is that it can store and release energy, but they do so in different ways, and at different points in the grid.

2.1.3 Grid Energy Storage

Grid energy storage, also known as Energy Storage Systems (ESS) can be utilised in various ways depending on the desired effect. A common use for ESS is load levelling. By storing power during periods of low load, the power can be supplied at a later period during high load. This brings economic benefits, as off-peak prices are lower than peak prices. An additional benefit of load levelling is reduced need of grid upgrades, as the total loads are going to be lower. A similar method to load levelling is peak shaving, where peak demand is lowered by supplying power from the ESS system when needed. This will also tend to lower prices for the customer[76].

Another important use of ESS is frequency regulation and maintaining spinning reserve. Installing more VRE sources will lead to increased variability and intermittency of the power sources, which means that the grid frequency will shift more than with conventionally powered grids. Additionally, a grid with high VRE penetration will have lower inertia, exacerbating the problem. By using fast acting ESS, the grid frequency can rapidly be corrected. A related issue is the topic of spinning reserve. In conventional power plants, generators are required to keep a certain idle capacity in case of outages. By using ESS, this is not needed, and the generators can run at more ideal power levels[61].

2.1.4 The connection between VRE penetration and ESS capacity

As previously discussed, building out more VRE to combat fossil fuel dependency and climate change brings with it several challenges related to power variability, frequency response, and security of supply. While ESS can be part of the solution to those aforementioned problems, investment into large scale deployment of ESS invariably involves the use of economic, energy and material resources. If the future energy mix includes a majority share of VRE sources, then the needs of adequate energy storage also needs to be taken into consideration to prevent the aforementioned issues. In essence: How much ESS is required of a given share of VRE penetration?

When discussing ESS requirements, two main figures are important. The first is the energy capacity requirement (Wh), and the other is the power requirement (W). There have been several studies on the relationship between VRE penetration and ESS power and capacity, 17 of which were analysed by Cebulla *et al.* The work mainly focused on the markets and geographies of the US, Europe and Germany[21]. For the study, the authors differentiated between grid types with different shares of PV or wind power. Based on the analysed studies, the authors remarked that grids with dominant shares of PV generally had a higher requirement for ESS capacity and power than grids with higher shares of wind[21]. The main reason for this was cited to be the spatial distribution of solar PV over a limited geographical region, for example in the case of Europe. As PV panels do not generate power at nighttime, this geographical issue necessitates larger capacity ESS to compensate than for large scale deployment of wind power[74]. In theory, a solar powered grid could circumvent this drawback by being spread over a large geographical area, but a complete substitution of ESS requirements is unlikely unless a fully global power grid is implemented[21].

Cebulla *et al.* observed different behaviours of required ESS power and ESS capacity with increasing VRE penetration. A common trait between the analysed studies was that ESS power requirements increased relatively linearly with VRE penetration, while ESS capacity requirements increased exponentially for the researched locations[21]. However, the results also showed signific-

ant variations, depending on the study being analysed and share of wind or solar PV. This was specifically evident in terms of ESS capacity. For the studies focused on the US and Europe and VRE shares over 80 %, a capacity requirement of 1.0-3.0 TWh for PV-dominated grids and 0.2-1.0 TWh for wind-dominated grids[21]. The authors also took grid modelling into account, but came to no general conclusion on how it affected ESS requirements. However, ESS requirements were observed for gird models with large amounts of transmission abilities, and vice versa. The authors remarked that real life storage requirements would be higher than forecasted by the analysed studies.

A study by Zsiborács *et al.* also investigated a similar relationship between VRE penetration and ESS power and capacity. For the study, the challenges of European VRE integration was examined, as well as the influence of VRE penetration on ESS requirements. The basis of the study was three scenarios by the European Network of Transmission System Operators, towards the year 2040, examining the different requirements of VRE deployments for each specific scenario. The authors devised a polynomial regression model in MATLAB by combining the logic of seven studies, which were themselves meta-analyses of hundreds of studies[89]. The developed model demonstrated the relationship between VRE penetration and the energy storage fraction for the European market towards 2040. The model assumed other measures than just ESS integration was implemented, and that demand side management, weather forecasting and network development was performed as well. The result of the analysis is displayed in Figure 3

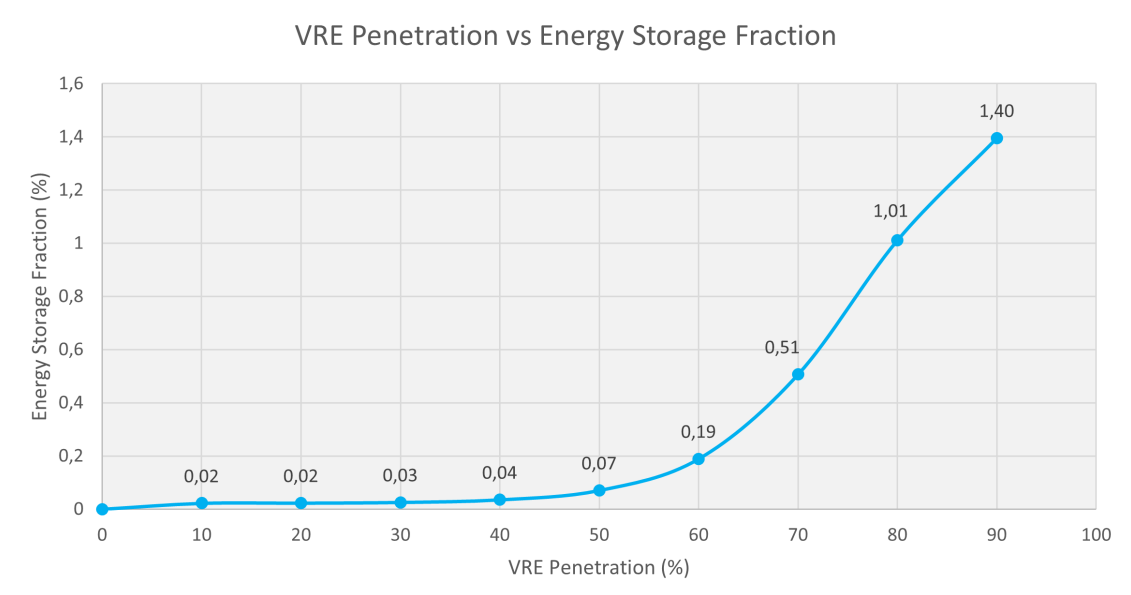

Figure 3: The energy storage fraction, i.e the percentage of electricity demand which is required for storage, versus the corresponding VRE penetration. Results from Zsiborács *et al*[89].

By multiplying the energy demand (In TWh) with the storage fraction, the demand for ESS capacity could be obtained. The model showed a relatively linear increase in storage fraction until about 45 % VRE penetration, and then a sharp increase. At VRE penetration above 90 %, the deviations between different studies was regarded as too significant[89].

2.1.5 Common types of ESS

There are a multitude of different ESS available on the market today, based on several different technological principles. This thesis will mainly focus on electricity storage systems, which store electrical energy by converting it into a different form of energy to store energy (charging), and then converting it back to electricity to discharge. There are several ways to achieve this conversion:

Pumped Hydroelectric Storage. Today, the largest amount of energy stored in ESS consists in the form of Pumped Hydroelectric Storage (PHS)[45]. PHS plants consists of two water reservoirs of different elevation, which are connected via a penstock and hydroelectric turbine, relatively similar to a conventional hydroelectric power plant. The key difference is that the turbine is designed to work as a pump as well, so that the plant will consume power during off-peak hours to pump water from the low reservoir to the high reservoir, and produce power during peak hours by running as a conventional hydroelectric plant. PHS has a conversion efficiency (I.E. the total efficiency from storing to releasing its energy) of around 65-80 %, depending on different factors[59]. PHS allows to store vast amounts of energy relatively cheaply, but has a prime disadvantage of needing water reservoirs at different heights, which often makes it dependent on favourable geography.

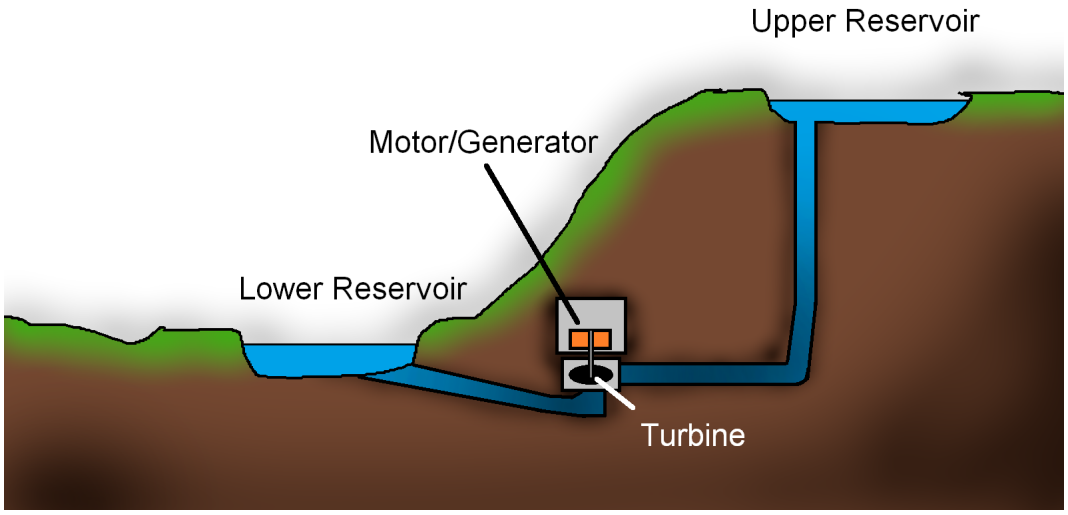

Figure 4: Simplified schematic of a pumped hydroelectric storage plant. The water can be pumped from the lower reservoir to the top to charge the system, and discharged by working as a conventional hydroelectric plant.

Thermal Energy Storage. Another ESS system which can be widely used is Thermal Energy Storage (TES). TES systems can be classified by two modes of operation: Sensible heat storage and latent heat storage, of which the former stores thermal energy as a function of temperature, and the latter primarily stores energy through the phase transition. The storage medium used in TES can be many different materials, like water, salt, rocks or others. TES can be both used to store heat energy and electric energy. In the latter case, the stored heat energy has to be harnessed through a heat engine[6].

Compressed Air Energy Storage. Compressed air energy storage, or CAES, works on the principle of storing electrical energy by compressing air in tanks or underground caverns. The air can then be released, heated up, usually by natural gas, and spun through a turbine to discharge the system and deliver power to the grid. CAES is relatively low cost, can store energy for a long time, and has limited material use. The disadvantages of this system is that it has relatively low efficiency of 40-52 %, due to heat lost during compression. It's also reliant on natural gas, which is a fossil fuel[47]. Another type of CAES is developed by SINTEF, where the compressed air releases its heat in a heat cavern, which is then transferred to the discharging air, leading to increased efficiencies of up to 70-80 %[4].

Battery Energy Storage Systems. Rechargeable (or secondary) batteries are one of the most used systems for storing electrical energy, and their application for grid energy storage will be the main focus of this thesis. They function as electrochemical cells, which utilise redox reactions to either store or release electrical energy[19]. Unlike many other forms of ESS, batteries operate with near instant response, produce electricity directly without the need for mechanical conversion, and produce neither noise or harmful emissions during operation.

2.1.6 Types of Battery Energy Storage Systems

BES systems can be classified by many different parameters, but a practical way to differentiate between systems is by their market sector. In a literature study on battery stationary storage in Germany, Figgener *et al.* split the BESS market into three sectors: PV Home Storage Systems (HSS), Industrial Storage Systems (ISS) and Large-scale Storage Systems (LSS)[34]. The different markets dictate important parameters for the BES system in terms of desired application, energy capacity, voltage level, power output and its relationship to the rest of the power grid. The latter allows the BESS to be classified into so-called "behind the meter" (BTM) or "in front of the meter" (FTM)-systems. This section will give an overview into different types of BES systems and how they work.

HSS systems are examples of so-called "behind the meter"-applications (BTM), ESS which are typically installed in homes or small businesses. They have a low capacity and power output, but are typically scaled to match the customers needs in terms of power and capacity. As the system is connected to the home, voltages are typically low as well. In HSS systems, the grid operator have limited insight into the system operations. HSS systems are often combined with domestic installation of solar PV, which allows the customer to store the energy generated by the solar panels when its not used, which increases self-reliance and lowers electricity prices for the customer. Some utilities will also allow surplus power to be sold back to the grid, making a HSS system particularly attractive. One major advantage of HSS combined with PV is that it allows expansion of renewable energy without needing to do changes to the power grid.

ISS systems can typically be installed either BTM or FTM, and are used for a variety of industrial applications, but common uses include peak shaving, UPS, or storing energy for EV charging. Unlike HSS systems, ISS systems can be connected to either the medium or low voltage network, depending on function. If connected to the low voltage network, the ISS system usually works BTM, while the opposite is true if connected to the medium voltage network. In the latter case, the system can perform frequency regulation. ISS systems are defined by Figgener as having power

levels up to 100kW and capacities up to 100 kWh[34].

Up in scale from ISS systems, there are LSS systems. These are systems with power levels up to 10 MW and 10 MWh capacity, which are installed in front of meter-applications. They are consequently connected to either high voltage or medium voltage networks, and usually perform frequency regulation and other typical FTM-duties.

2.2 Energy Storage using the Lithium Ion Battery

The battery type which will be the main focus on this thesis is the lithium ion battery (LIB). The LIB is currently the most popular type of battery for ESS applications. As the LIB has become popular in other markets, mainly personal electronics and BEVs, spillover effects have caused the LIB to dominate the ESS market too, particularly due to lower costs, as well as higher specific energy and longer cycle life than previous battery technologies[63][45].

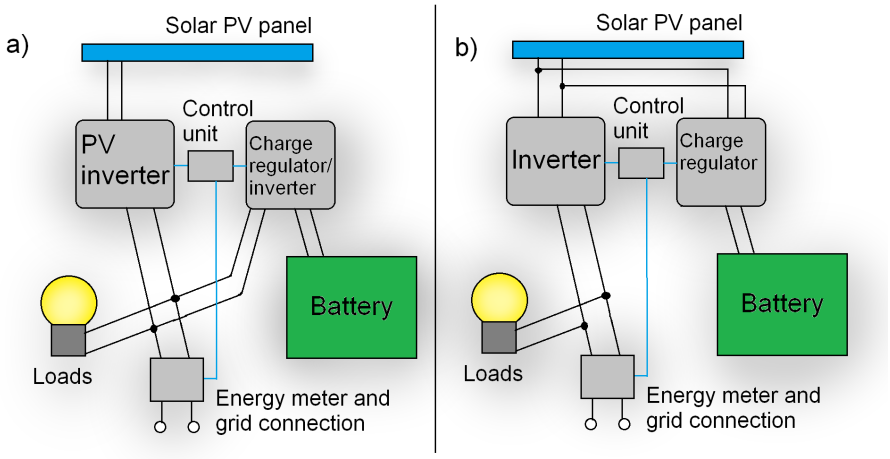

Figure 5: Schematics of (a) AC coupled and (b) DC coupled residential ESS. Black lines indicate power transmission, blue indicates control unit connections.

2.2.1 Lithium Ion Battery Energy Storage Implementation

LIB based BES systems can have a variety of different layouts depending on the capacity, mode of operation, and other factors, and there are many different systems available which vary greatly in their design. However, most BES systems still consist of similar components, no matter the capacity and function of the system. The main differences manifest themselves in terms of scale and relationship with the rest of the power grid. A such, there exists differences between residential scale BES systems and utility scale BESS, for example.

The common denominator for all LIB based BES systems is the battery cell. The cell is the basic unit of any lithium ion battery, and consists of an anode (negative terminal), cathode (positive terminal), separator and electrolyte. Depending on the format, the cell can be pouch-shaped, cylindrical, or prismatic. A more detailed overview of the battery cell is performed from Section 4.3.2 onwards. The next unit is the module, which is a structure containing a fixed number of cells which protects the cells from external disturbances. The final unit is the pack, also called a rack by some BESS manufacturers. This contains a number of modules combined with supporting

systems like battery management systems, cooling systems, etc[78][70].

As discussed earlier, residential, or home storage systems (HSS) usually integrate with domestic solar PV panels, although this isn't necessarily a requirement. When PV integration is used, the main PV home storage systems used today can be classified as either AC coupled or DC coupled systems[83]. As both the battery and PV panel work with DC voltage, the energy either produced or stored needs to be converted between the frequency and voltage supplied by the electric grid to the required DC voltages. This is achieved by using solid state inverters. In the AC coupled system, the PV supplied power is first converted from DC to AC to supply the loads in the building or supply power to the grid. For charging the battery with PV, the power needs to be converted back into DC by supplying it to a battery specific inverter. This involves converting from DC-AC-DC. Another system, called DC coupling, uses a single inverter to supply both the battery and the loads or grid, which only involves AC-DC (or DC-AC) conversion. This has a higher conversion efficiency than the AC coupled system[56]. A schematic drawing of both types of systems is shown in Figure 5

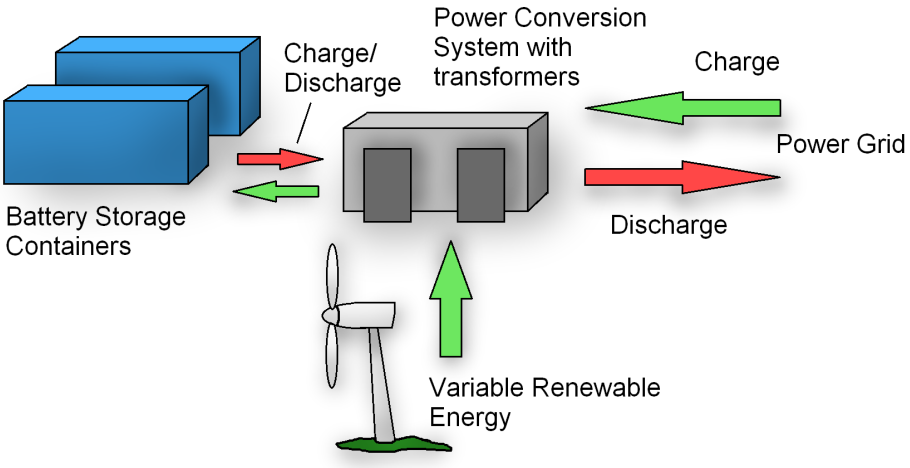

Figure 6: Schematics of a utility-scale LIB BESS system connected to VRE generation through the use of a Power Conversion System.

Larger systems work on the same principles as smaller systems, but on a larger scale. While a HSS system will typically consist of one single pack, a larger scale ISS or LSS system can be made up of many racks interconnected. A common format is containerised BESS. This groups the battery racks into standard ISO intermodal containers, allowing for simple transport, integration of air conditioning systems and a minimum of on-site work to install the system[70]. A grid-connected LSS typically delivers and receives three phase, high voltage power. This requires auxiliary systems like transformers, which may necessitate a more area-consuming layout than ISS or HSS systems. These systems may be containerised themselves. In this arrangement the BESS containers are connected to a container-based power conversion system (PCS), which consists of transformers, inverters and other control systems. The PCS is then connected to the grid and potentially directly to VRE sources like wind turbines and solar panels, as shown in Figure 6. The electrical layout can still be either AC or DC coupled[43][56].

2.3 Lithium Ion Battery functionality

This section will introduce the basic functionality of how a lithium ion battery works. The battery consists of two electrodes connected to their respective current collectors, separated by a separator layer. In between the electrodes there is a liquid electrolyte that allows for migration of lithium ions, but not electrons. The anode side of a typical lithium ion battery consists of carbon, often in the form of graphite, connected to a copper current collector[71]. On the cathode side, an aluminium current collector is connected to the active cathode material, which is usually made from a lithium transition metal oxide[71]. The separator allows lithium ions to pass through itself and is usually made from fibreglass or polymers. The function of the separator is to keep the anode and cathode to come into direct contact[19].

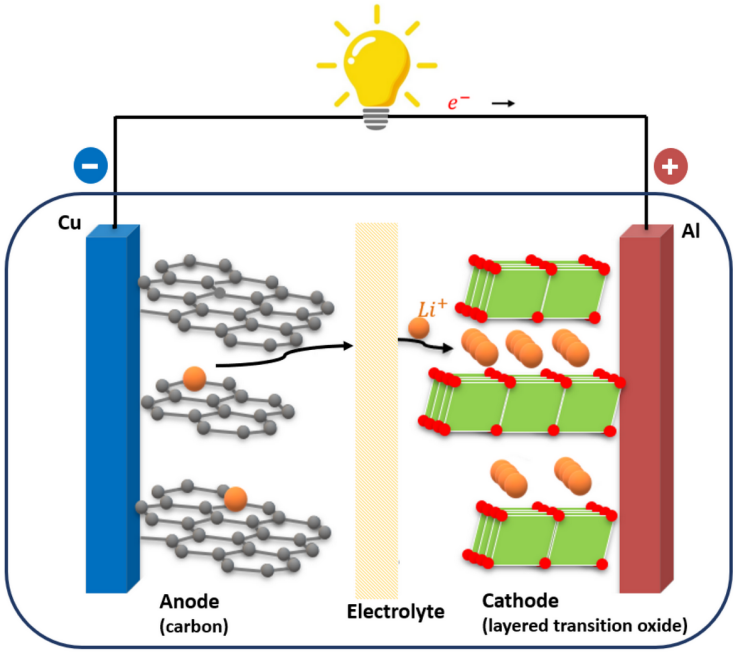

Figure 7: Basic functionality of a lithium ion battery with a graphite anode and a layered transition metal cathode. Figure by Spitthoff *et al*[71].

When the battery is charged, li+ ions are depleted from the cathode. They then move through the separator and into the anode, where they are stored between the graphite layers after receiving electrons from the external circuit. This process is known as lithiation. When the cell is discharged, the anode gives away its lithium molecules and electrons(delithiation), reversing the process. When the cell is charged and discharged for the first time, some of the electrolyte forms a passivating layer on the anode surface, which is known as the solid electrolyte interphase (SEI)[10]. An overview of a LIB with $LiCoO_2$ cathode and graphite anode is shown in Figure 7. A commonly used term for describing charging/discharge current is C-rate. If a battery charges at 1C, that refers to a charging time of 1 hour from 0% state of charge (SOC) to 100%. 2C then indicates a charging time of half an hour for the same battery[19].

2.4 Chemistry Types and Formats

While the lithium cobalt oxide battery was the first type to be developed, many other types of LIB chemistry have later been developed. This section will briefly introduce some of the most popular anode and cathode chemistry types in use today.

2.4.1 Anode Chemistry

Most commercial LIBs are equipped with anodes made from carbon in some form. The most used type is graphite, but hard carbon can also be used. Graphite has a layered structure, while hard carbon has a randomized structure. Some of the reasons for using carbon is that it is relatively cheap and has a low degree of expansion when lithium molecules are inserted (lithiation). Significant research has been performed on using silicon as an anode due to its larger specicif energy, but it suffers from expansion during lithiation, which cracks the SEI layer and leads to reduced lifetime[71].

2.4.2 Cathode Chemistry

Lithium Cobalt Oxide. Lithium Cobalt Oxide was the earliest cathode chemistry to be developed. It is a layered structure consisting of $LiCoO_2$ and is generally characterised by a high theoretical specific energy density of 150-200Wh/kg and nominal voltage of 3.60V[18]. The biggest drawback is the use of cobalt and the structural stability of the cathode structure at high degrees of lithium depletion. This means that commercial LCO cells typically only have half the capacity of its theoretical maximum[19]. Due to it being the first type of LIB to be developed and because of its high specific energy, it has traditionally been used for portable electronics, but it is starting to be replaced by other chemistries because of safety concerns[90].

Lithium Manganese Oxide. Another type of cathode chemistry developed was LMO, based on $LiMn_2O_4$. This is based on a spinel structure. LMO has a voltage of 3.7V. LMO exhibits good safety characteristics, but struggles in terms of specific energy density, having 100-150Wh/kg. LMO can be mixed with nickel manganese cobalt to improve this.[18].

Nickel Manganese Cobalt. Partly because of the previously mentioned problems with the LCO cathode, other batteries have been developed. One of the more promising technologies is the Lithium Nickel Manganese Cobalt Oxide ($LiNiMnCoO_2$), or NMC. NMC utilizes a layered structure similar to LCO, has a nominal voltage of 3.70V and a relatively high specific energy of 150-220Wh/kg[27][18]. There are several different types of NMC cathodes, all distinguished by the different fraction of either Nickel, Manganese or Cobalt. NMC111, NMC622, NMC811 and so on. While Nickel rich NMC cathodes have a high capacity, they also have lower thermal stability and cycle life[27]. It is also a goal to reduce the fraction of cobalt in the cathode, as this is a conflict mineral and is also expensive. Still, the NMC chemistry is one of the most commonly used in electric cars.

NMC111. As the name suggests, NMC111 is made from Lithium Nickel Manganese Cobalt or $LiNiMnCoO_2$, with 33 % of each component of Ni, Mn, and Co. This is the most common type used in EVs today[27].

NMC622. Both cost and performance reasons drive the amount of cobalt and manganese down in more recent developments of the NMC chemistry. One of these developments is the NMC622 type. The higher relative amount of nickel increases capacity and lowers cost[27].

NMC811. A further development of the NMC622 concept is the NMC811. Here, the manganese and cobalt have been further reduced. This increases capacity and lowers cost even more, and this means NMC811 is a very promising technology in the short to mid term future[27].

Nickel Cobalt Aluminium. Another cathode chemistry based on nickel and cobalt is Lithium-Nickel Cobalt Aluminium. In similarity to LCO and NMC, this is also a layered structure and consists of $LiCoAlO_2$[18][27]. NCA is characterized by a high capacity of 200-260Wh/kg, the highest for the chemistry types discussed here. However, it can suffer from thermal instability[16].

Lithium Iron Phosphate. Another relevant cathode chemistry is LFP, based on Lithium Iron Phosphate ($LiFePO_4$). Unlike NMC and NCA, the chemistry is not based on either nickel or cobalt. LFP cathodes exhibit good structural and thermal stability at high SOC. This is mostly resulting from the olivine crystal structure[48]. Compared to NMC or NCA, LFP based batteries have great safety advantages in their low self heating rate[16]. LFP typically has a specific energy of 90-140 Wh[90]. This is typically lower than in NMC or NCA cells. LFP still have other advantages, especially in terms of cycle life; typically up to 2000 cycles[18].

2.4.3 Cell Formats

Pouch. An important consideration in battery design is how to contain the cell materials and isolate them from the environment. Lithium ion batteries need considerably more advanced packaging, in order to seal the electrolyte and active materials from reacting with atmospheric oxygen. This packaging is typically called cell format or geometry. For LIBs, formats can typically be split into two categories: Hard case or soft case. Hard cases concerns prismatic and cylindrical cells, while soft cells mainly regard pouch cells. This section will describe the differences and primary advantages of each cell type.

The most common cell format today is the pouch cell. In this type, the active materials are stacked on top of each other and contained inside a thin foil commonly called the laminate. The foil is usually two separate pieces welded together to form an air tight package. The electrolyte is then injected and the fill-hole is sealed[40]. The pouch cell has several advantages: It's the most packaging efficient cell format, it can be flexible and can be formed into a wide variety of sizes and shapes[44][18]. This makes it relatively easy to integrate them into modules of a desired shape and size, which gives more degrees of freedom in the design phase. It is therefore popular in portable electronics, electric vehicles, drones and other applications that favour these properties. It also has disadvantages; The cell needs a physical case to protect it, as the laminate lacks the structural

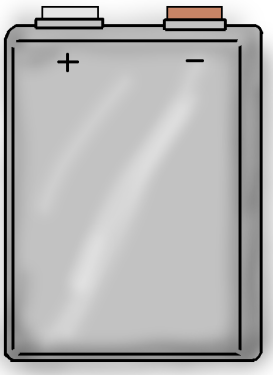

Figure 8: Pouch cell.

integrity to protect the cell from any higher mechanical force. It's also susceptible to swelling if there is internal gas buildup[44][18].

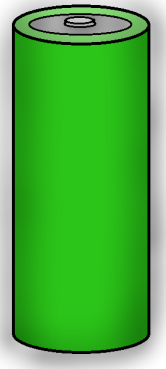

Figure 9: Cylindrical cell.

Cylinder. Another common format is the cylinder. This is a type of hard case, that contains the active materials in a hard, cylindrical outer metal casing. In the vast majority of available cell designs, the dimensions are standardised, allowing the cells to be mass produced. An example is the ubiquitous 18650 format, which is widely used by many different applications. The naming convention is derived from the cell width and length, in this case 18mm width and 650 mm

length.[44]. The cylindrical LIB is produced differently from the pouch cell. Instead of having the cells stacked on top of another, the cells are winded into a roll-like shape called a jellyroll. This is then inserted into the casing[40]. To build on the previously mentioned advantages of standardisation, cylinder cells are very easy to integrate into a module or pack. They can also achieve a high power density, and there are many different capable manufacturers to choose from. There are disadvantages too; Cylindrical cells can have a lower energy density on a module and pack level than a typical pouch pack, as the individual structural casings account for extra mass, and there will be an air gap between each cell[18]. In addition, modules and packs have a lower limit on their thickness.

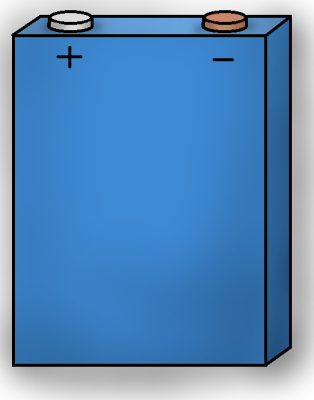

Figure 10: Prismatic cell.

Prismatic. Another hard case-type format is the prismatic cell. These consist of the active materials, either in a jellyroll or stacked, contained in a hard, prismatic shaped case, often made from hard plastic or metal[44]. The prismatic cell is less popular than either the cylinder or pouch, but it's still used in portable electronics, electric vehicles and other applications. It's prime advantage is simple packaging, as it can be easily stacked into modules with simple manufacturing. The cell loses attractiveness in other points, due to lower energy density compared to the others, lower thermal conductivity and some swelling issues[18].

2.5 Mining, Materials and Manufacturing

Although the basic components of the lithium ion battery have been described, for calculating the environmental and resource impact of future LIB ESS demand, an accurate picture of the production process is required. A large share of greenhouse gas emissions and environmental impact of LIBs is related to production phase processes. While the current environmental and climate impact of LIB production is relatively limited at a global scale, if future demand increases dramatically, this impact will no longer be negligible. The LIB production process can be divided into three parts: Mining and refining, battery material production, and cell production and battery pack

assembly. [32]. This section will give an overview of each step and discuss relevant environmental consequences.

2.5.1 Mining and Refining

The first step of producing any battery is to obtain the required materials that make up the battery. In the case of the LIB, these materials take the form of minerals and metals that need to be mined. The materials for LIBs are usually sourced from several sites around the world, depending on the material. As the LIB market expands, material concerns become larger, and the right choice of chemistry becomes even more important in regards to cost and availability. This section will explain how the most relevant LIB materials are obtained, and some of the environmental issues relating to the mining processes.

Lithium. Lithium is the common metal for all LIB chemistries. Over 50 % of the global lithium reserves are located in Argentina, Bolivia and Chile, known as the so-called "Lithium Triangle". The conventional way to extract lithium is through brine pools, where brine from lithium rich regions is pumped from the ground and allowed to evaporate in large, open air pools. When the water is sufficiently removed, lithium chloride (LiCl) remains for further processing. Another way is to mine the lithium from rock ores. This method is much more complex than the brine method, which necessitates that the mining process is adapted to the local deposit's chemical and physical composition[49][57].

Graphite. As it's currently the most common type of anode material for LIBs, graphite is also an important material for LIB market growth. Graphite can be classified as either natural or synthetic, wherein the natural type is mined as ore, while the synthetic type is a petroleum product, created from heat treatment of coke or tar[53]. The lead producer of natural graphite currently is China, with 67 % of the global market as of 2017[67]. Synthetic graphite is usually the most usable for battery anode applications, as it's exhibits higher purity. As of 2020, around 50:50 of the graphite used for LIBs is synthetic, but this is expected to rise to about 70 % in 2030, according to Wood Mackenzie[75].

Nickel. For common LIB chemistries like NMC and NCA, nickel is an important material. Nickel is usually present in two different types of ores; Sulfide or laterite. Typically, sulfide ores have been the principal source of nickel, in either open cut or underground mines. The ore is then concentrated by flotation and smelted to produce nickel. This process is relatively similar to other metals. On the other hand, the processing methods for laterite-sourced nickel are more complex[58]. The three largest nickel producing countries (as of 2022) are Indonesia, the Philippines and Russia[64].

Cobalt. For NMC and NCA, another critical cathode material is cobalt. Most of the global cobalt production comes as a byproduct from copper or nickel mining, except for production in Morocco and the DRC (Congo), for the latter in case of artisinal mining. The DRC is the world's largest supplier of cobalt, and 10-30 of the country's production is mined artisinally under harsh conditions, presenting a large ethical concern[80]. According to Zubi *et al*, cobalt is already in critical supply, as the battery industry already consume around 30 % of the global cobalt market. With future

production, this is expected to increase to 75 % in 2025[90]. Moving towards chemistries containing less cobalt, or removing cobalt altogether is therefore of great importance for the battery industry.

Phosphorous. In LFP batteries, phosphorous is used in the cathode material. Phosphorous is usually produced from mining phosphate rock through either a wet process or thermal process. The vast majority of phosphorous is consumed by the agricultural industry as fertiliser, but as LFP increases its market share, the battery industry will also increase its consumption accordingly. Phosphorous is listed as a critical material by the European Commission[35].

2.5.2 Electrode Material Production

After the raw materials have been obtained, the electrode active material needs to be processed and produced. The active material is usually delivered in powder form to the production site. The production methods varies between different manufacturers and chemistries, but general similarities can be observed. In the case of LFP, several different methods can be used, usually separated between 'solid state' or 'solution-based' methods. Solid state methods involve using mechanical processing, like pelletizing, grinding and dry mixing to process the precursor materials. The materials are then calcinated, which is a heat treatment process which occurs at high temperatures. After calcination, the material is grinded into a fine powder, resulting in the final $LiFePO_4$ product. Because solid state methods have reactions taking place in the solid phase, temperatures required are high, the processing time is long, and repeated grinding is necessary. This makes it energy intensive and expensive, and less ideal for mass production. Additionally, the electrochemical performance is not ideal, and particle sizes are large[79].

Partly because of the aforementioned reasons, solution based methods have been developed, which are of increasing importance. Examples of solution based methods include hydrothermal synthesis and co-precipitation. In the former case, the precursor solutions and a surfactant is mixed at the stoichiometric ratio, then heat treated in an autoclave at around 120-220 degrees C for 5-10h. The product is then dried to create the finished $LiFePO_4$ powder. In hydrothermal synthesis, calcinating is not nessecary unless a carbon coating is desired[79]. In co-precipitation, the mixed precursor solution is precipitated by controlling pH values. The slurries are then filtered, washed and dried. To obtain crystalline $LiFePO_4$, the material is calcinated at 500-800 degrees under an N2 atmosphere. Co-precipitation is easy to control and the finished product has a high purity and small particle size[79][88]. NMC active material production also uses a similar process with co-precipitation and calcination. According to Dai *et al.*, multi-stage calcination was needed for automotive grade batteries, which would lead to higher energy use during material production than reported in other literature[24].

2.5.3 Cell manufacturing and pack assembly

The cell production process consists of several steps which are described here, as well as shown in Figure 11. The process can differ by manufacturer, so this section is intended as a general overview.

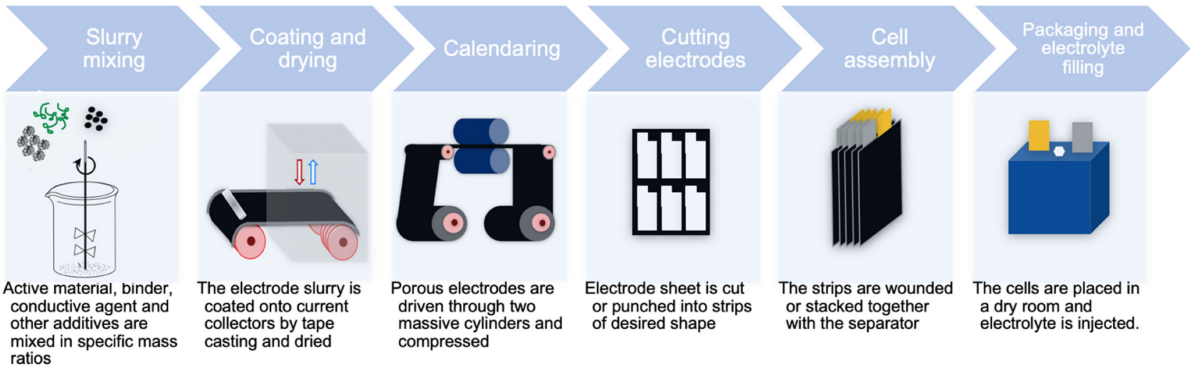

Figure 11: A general overview of the cell assembly process of a typical lithium ion battery. Figure by Brynesen *et al*[17].

Mixing. The components, including binders and active materials of the cathode or anode are mixed together with solvent, creating a slurry which is loaded into storage tanks. An alternative process is to use mix the components in an extrusion device. This process has the advantage of being continuous, removing the intermittent step of using a storage tank.

Coating. The slurry is coated onto the current collectors of the anode or cathode, made from copper and aluminium respectively. If the storage tank method is used, the coating step will be integrated into the extrusion device.

Drying. After application of the active material, the foil is brought through the drying chamber. In the case of the anode, the active material is a wet film, a homogeneous mix of solvent, graphite, binder and carbon black. When drying, this layer will gradually thin and the solvent will vaporise. Firstly the now thinner layer will act as a capillary network. Then the liquid will be partially removed, and then will be removed completely, leaving a dry surface. Drying is one of the most energy-intensive steps of the cell assembly process[32].

Calendering and Slitting. The foil is statically discharged and compressed by rollers. Pressure needs to be precise in order to not crush the electrode material and get stress cracks. The foil is afterwards cut into smaller rolls (daughter-rolls) of similar width, either by shears or laser[40].

Cell assembly. This step differs from prismatic cells to pouch cells, although there are similarities too. For pouch cells, the foil is cut into the final shape, and the electrodes are stacked on top of each other together with the separator. The separator can also be folded between each electrode in a process called Z-folding. For cylindrical or prismatic cells, the process is slightly different, where the electrode foil is continuously winded together with the separator into a so-called "jellyroll".

Packaging and Electrolyte Filling. In this step, the cell is integrated into its packaging, a process which differs between pouch, cylinder and prismatic cells. For pouch format, the cell stack is inserted into a foil which has already been drawn into a pouch shape. The foil is then partly sealed by welding. The electrolyte is then filled into the cell, and the pouch cell gets fully sealed under vacuum. For cylindrical or prismatic cells, the jellyroll is inserted into an either cylindrical or prismatic housing instead. The electrolyte is filled into the housing, and the housing is sealed up[40].

2.6 Energy use and Greenhouse Gas emissions of LIB Production

A major concern regarding the transition toward mass electrification is the environmental impact of battery production. In the context of energy storage, the transition towards VRE sources and energy storage systems is primarily to alleviate the need for fossil fuels in power production, which will help to reduce the CO2 emissions and environmental impact of the global energy sector. However, the resulting environmental and emissions-wise consequences of large scale VRE- and following ESS installation cannot be ignored, especially if the VRE transition is supposed to fulfil its purpose of lowering greenhouse gas emissions. As discussed in Section 2.1, the required energy capacity of ESS installations could be described as scaling roughly exponentially with the VRE penetration. This means that the production intensity of ESS batteries will be exceptionally high at high levels of VRE penetration if grid stability and supply security is to stay at satisfactory levels. Minimising the production emissions, energy use and environmental consequences of BESS production processes is therefore of great importance for a large-scale transition towards renewable energy.

Emilsson *et al.* performed a literature study on the GHG emissions and energy use of lithium ion batteries used in light duty vehicles. According to the authors, energy use in mining was not well-reported. They cited a report by Argonne, where the only reported instance of energy measurements, more specifically in the form of diesel use, were reported in two cobalt mines, where one reported 163 kWh/ton mined ore of 0.32 % cobalt, while another mine reported 61.7 kWh/ton ore of 0.51 % cobalt[32]. According to a study by Wang Qi, based on data from the China Energy Statistical Yearbook, the raw material exploitation of the cathode materials $LiFePO_4$ (LFP), $LiCoNiMnO_2$ (NMC) and $LiMn_2O_4$ (LMO) would release 13 200, 18 200 and 11 600 kg CO2 eq per tonne of extracted material[82].

Emilsson *et al.* also concluded that the cathode material production had a significant energy consumption, and therefore GHG emissions, citing results from Dai *et al.* That study was mostly focused on NMC powder production. The authors found that NMC power production was energy-intensive, and that the co-precipitation step and calcination steps demanded especially high amounts of energy. However, a potential for lowering production energy intensity by utilising the capacity of the rotary kiln for calcination more efficiently. In summary, it was found that the production of the cathode active materials, in this case the NMC powder, contributed to 37 % of the material energy use for LIB production[24][32]. In a study by Hao et al., examining the production of LIBs in China, it was found that a significant share of the GHG emissions from producing either LFP, NMC or LMO batteries came from the cathode active material, contributing 48.4, 60.7 and 51.1 % respectively. However, the report also found large differences; studies conducted in the US showed a significantly lower intensity of GHG emissions for the active cathode materials[38].

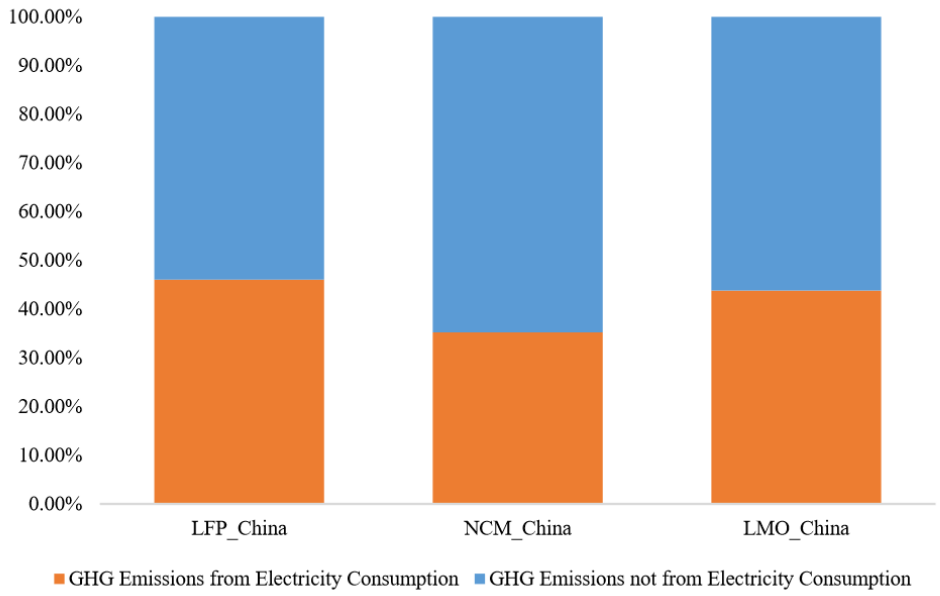

Figure 12: Percentage of GHG emissions resulting from LIB manufacturing attributable to electricity production. Figure by Hao *et al*[38].

When concering the cell production process, both energy intensity and GHG emissions vary greatly depending on the study. Ellingsen *et al.* examined the differing assumptions for several lifecycle assessments (LCA) of light vehicle traction batteries[31]. The authors found significant differences in the manufacturing GHG emissions, with the values varying from 38 to 356 kg of CO2 eq/kWh depending on which LCA was studied. The authors investigated the differences and concluded that the discrepancies happened due to differences in the assumptions for energy demand for production and material components. They also concluded that the chosen cathode chemistry did not significantly impact the total GHG emissions of the battery manufacturing. Ellingsen *et al.* concluded that the cell manufacturing was the single highest contributor to LIB manufacturing GHG emissions, and that using renewable energy in the energy-intensive parts of the process would contribute to lower GHG emissions[31]. Similar results were also found by Hao *et al.*, where the GHG emissions from electricity useage for LFP, NMC and LMO batteries were found to be 46.1, 35.2 and 43.8 % respectively[38].

In Emilssons study, the largest contributor to the cell manufacturing energy useage was found to be the electrode drying and dry room steps, contributing to 39 and 43 %, respectively. For the dry room conditions used in cell assembly, this was found to be region specific. In regions where hot and humid climates dominate, the energy use for dry rooms was found to be significantly higher than for colder climates[3][32]. The other significant energy use component was the electrode drying process. According to Wood *et al.*, the electrode drying process is dependent on the type of solvent used. NMP demands a higher energy use for drying than water, as the flammability of the solvent requires high amounts of heated airflow to both evaporate it and keep it from reaching flammable concentrations It is therefore possible to reduce the energy intensity of electrode drying by changing the solvent to water for either the cathode, anode or both, and water is commonly used already for anode production[84]. However, there was no indication that was water was presently used as a cathode solvent in production plants[32]. Another alternative is to use electrode material

without the need for solvents in the first place, known as semi-solid electrodes[17].

In summary, it was found that LIB production is an energy intensive process, and that a large share of the greenhouse gas emissions came from the energy use, especially from the electrode drying and dry room facilities. The production of cathode active materials were also found to take a large share of the total GHG production emissions. In Emilssons study, a LIB production GHG emission intensity from 59 to 119 kg/kWh of battery was found, depending on if the energy use was renewable or not[32]. Ellingsen *et al.* identified a range between 38 to 356 kg/kWh for the same value, but not all the LCA studies analysed by the authors were identified to have the same assumptions, which would impact the final values greatly[31]. Hao *et al.* estimated values of 109.6, 104 and 96.6 kg/kWh, depending on if the cathode chemistry was LFP, NMC or LMO[38].

2.7 Critical Materials

As the global LIB market becomes larger, the material usage of LIB production becomes more problematic. Especially as both the automotive, personal electronics and ESS markets are destined to grow dramatically in the coming decades, the usage of LIB materials is also going to grow at a similar rate. Several of the materials already in use for LIBs already suffer from low availability, high prices, or unethical extraction methods. While the ESS market does not currently suffer from material shortages, the combined effects of all markets growing can lead to great uncertainties for the future. The growing market can also lead to uncertain environmental consequences due to the extraction of virgin materials.

The most serious current material issue is cobalt, which is used in the cathode chemistry of NMC, LCO and NCA chemistries. These types are most commonly used in BEVs and personal electronics due to their favourable characteristics like high specific energy, but they have also been frequently used in ESS. The global cobalt reserves, as of 2021, are 7.1 million tonnes, and there is growing concern that the increased demand for cobalt-containing LIB types will lead to supply chain issues[90][77]. Cobalt can be both produced as a byproduct of nickel and copper production, or mined directly in geographic locations where that is possible. The biggest producer of mined cobalt is Congo (DRC). The country is plagued with political instability, human rights violations and other societal issues. Additionally, around 10-30 % of the cobalt in DRC is mined artisanally, which is unregulated mining, which often takes place in harsh conditions using manual labour, leading to human, societal and environmental consequences[69][36]. According to Zubi *et al.*, cobalt is already a critical material. Directly mined cobalt has the issues with concentrated, unethical production, and cobalt mined as a byproduct struggles with supply flexibility[90].

Lithium is a material which is absolutely necessary for lithium ion batteries. According to the USGS, the global lithium reserves are roughly 21 million tonnes, although total global resources are around 86 million tonnes. In 2020, global lithium production was at 82 000 tonnes. According to Zubi *et al.*, the lithium supply in the short and mid-term is not going to be critical, but that can change in the future[90]. There are also environmental consequences of lithium extraction. In evaporative brine extraction for example, water consumption is very high, which has led to depletion of groundwater reservoirs[49]. Graphite is another concern. While there is no current material shortage of natural graphite for battery applications, 65 % of the market is located in China. This has led to the US and Europe classifying natural graphite as critical material. While synthetic graphite is a possible replacement for the natural type, the production process involves

energy intensive steps and consists of precursor materials which are essentially petroleum products, with the environmental issues that entail[75][28].

The issues with material supply can be alleviated in various ways, and several measures have already been developed. As cobalt is currently the most critical material used in commercial LIB cells, battery manufacturers have started to move towards using less cobalt, or even eliminating cobalt altogether. This solution is conducted differently depending on the market. So far, cobalt reduction measures in the automotive sector have mainly focused on moving from cathode chemistries with high cobalt content towards ones with lower amounts. An example is the move from NMC111 towards NMC622 and NMC811, with each having lower shares of cobalt compared to the older chemistries. The reason for this is the higher specific energy of NMC cells compared to cobalt-free types like LFP. Bongarz *et al.* conducted an assessment of the future BEV and ESS market in Germany, and concluded that the automotive market would mainly use NMC cells towards 2050, but with higher nickel contents and lower cobalt use, citing a gradual move towards NMC811 as the dominant technology. In their assessment on the German ESS market, they regarded LFP to be the dominant technology until 2050 in their conservative scenario. However, in their "innovative" scenario, they estimated an eventual increase in more advanced battery technologies, leaving lithium sulphur (LiS) and lithium-oxygen (LiO) as the dominant technologies[14].

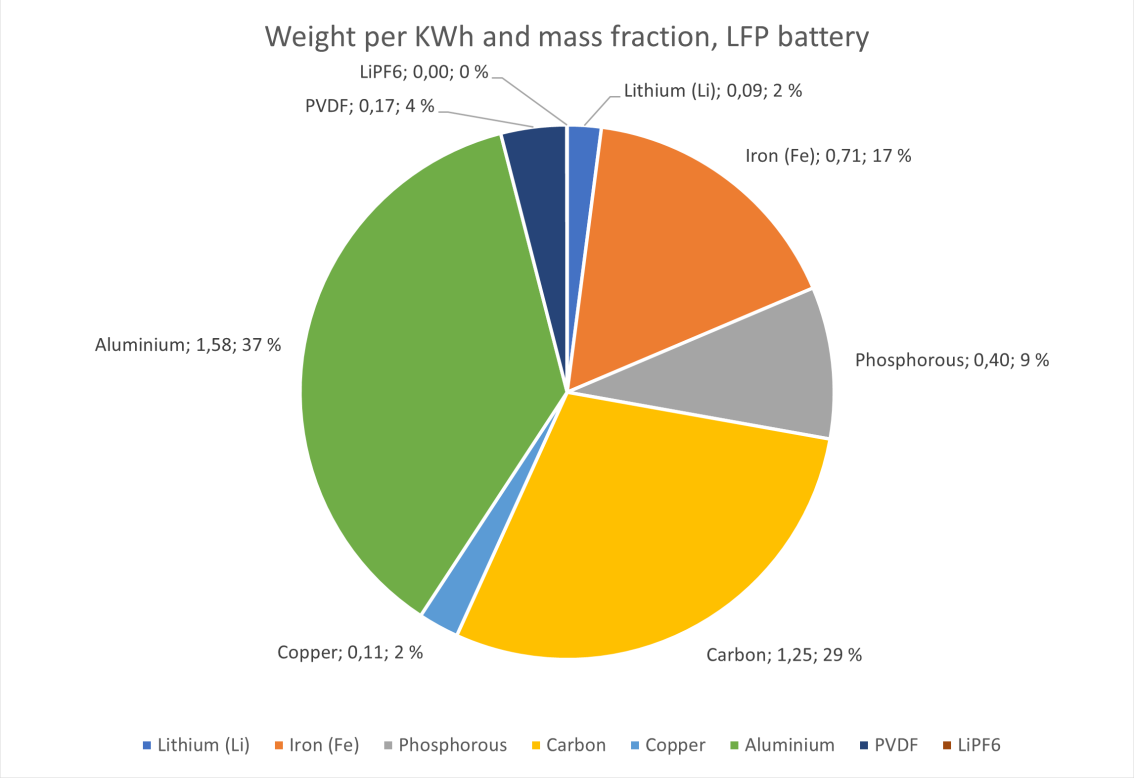

Figure 13: The weight per KWh and mass fraction (in %) for each component in a LFP-based lithium ion battery. Values were calculated by BatPaC[9].

Another crucial way to lower the use of critical materials is to establish a full circular economy in the lithium ion battery market. This can be done two ways: Second life use and recycling. The second life solution involves to reuse batteries in other applications than they were originally intended. A common method is to reuse BEV batteries that have degraded beyond their usefulness to be repurposed for other uses, commonly for ESS, where the full capacity range may not be as necessary. For example, in Germany, BMW i3 batteries were repurposed to act as stationary

energy storage batteries[12]. This has the advantage of "dilluting" the environmental impacts of the battery's production by using it for a longer time, and provides a cheaper source of batteries for several sectors. However, there are still challenges with second life use. A battery produced for BEV usage is typically designed to have high specific energy, while a BESS battery will typically need to be designed for lower cost and high cycle life, as they will often need to be charged and discharged more often than the typical BEV and weight is not often an issue. This discrepancy means that a repurposed BEV battery may not last very long in a BESS setting, especially because it has already suffered degradation[28]. Another issue is that the reuse of BEV batteries will "delay" the eventual recycling of the battery materials. When reusing batteries designed for BEVs, the battery may for example be of an older NMC111 chemistry, which contains significantly higher amounts of cobalt than current types. Keeping the battery working for ESS applications would mean that the recycling of the battery can be delayed by several years, meaning that the expensive cobalt contained in the cells will not be recycled and potentially be used more efficiently in a more modern low-cobalt chemistry. Second life use therefore has potential to lead to increased use of virgin materials and supply issues[28][13].

Recycling of spent LIBs is another way to alleviate current and future material supply issues. Recycling can have positive environmental and economic effects, and can reduce the requirements of critical virgin materials. The most relevant candidate materials for recycling are therefore not surprisingly cobalt, lithium and nickel. Several different recycling processes exist, but the hydrometallurgical and pyrometallurgical methods have been the most successful so far[26]. The pyrometallurgical process involves a furnace which reduces the component metals of the battery into a slag part and a metal alloy part. The alloy part usually consists of nickel, cobalt, copper and iron, and can be reclaimed by hydrometallurgical processing. The slag consists of metals like aluminium, lithium, or manganese, which can also be further reclaimed by a hydrometallurgical process or used for other purposes. However, other components, like the plastics, electrolyte and lithium salts, are not recovered, and typically take up around 40-50 % of the battery weight. [39]. There are disadvantages with the aforementioned process. Firstly, pyrometallurgical process is energy intensive, and secondly not all materials are reclaimed. There are other recycling methods available, but so far there are challenges with finding a recycling methods that is both energy efficient, reclaims all important battery components, and is commercially and environmentally sustainable at the same time.

2.8 Lithium Ion Battery Ageing

One of the most relevant problems facing LIB adoption is ageing. All LIBs lose performance over time, and minimising this downside is important, especially for applications that require longer life, like BEVs and power systems. The cause of ageing can be related to two factors: Loss of lithium inventory (LLI), and loss of active material (LAM). LLI results from SEI decomposition, electrolyte decomposition and lithium plating[71]. LAM is caused by the active material dissolution, structural deterioration of the electrodes, and other factors[71].

2.8.1 Cycle Ageing

For the anode, which is commonly made from carbon, several different processes occur which degrades the life of the battery. Two of these relate to changes in the electrode/electrolyte interface.

When the battery is first charged after manufacture, a SEI film occurs on the anode. This can already consume up to 10 % of the active lithium ions, leading to reduced capacity. In addition to the SEI film, another, perhaps more serious issue is the buildup of metallic lithium on the cathode. This metallic lithium will form as structures called dendrites and can grow large enough to puncture the separator, leading to a short circuit. This can be severely dangerous, leading to a thermal runaway and potentially starting a fire[86]. The formation of lithium plating is generally a problem at high charging rates or during overcharging[85].

Other mechanisms relate more to attenuation, or weakening of anode materials. This generally results from mechanical and structural failure of the anode from the insertion and removal of lithium during cycling as well as gas escaping from anode reduction reactions. This contributes greatly to degradation. In addition, the change in volume leads to cracks in the SEI film, which in turns means more SEI will generate, leading to even more capacity loss. These problems also lead to increased ohmic resistance during operation[85].

The cathode is made from different lithium metal oxides depending on chemistry. Here, the main processes which contribute to ageing are dissolution of the cathode material, the destruction of the cathode structure and phase transition[85]. The dissolution is the most contributing factor to battery degradation, primarily because the dissolved products migrate to the cathode. This adds to a CEI(cathode-electrolyte interphase) film. The CEI usually doesn't cover the entire cathode, and is also thinner than the SEI layer on the anode. Xiong *et al.* found that this effect is most pronounced in manganese electrodes, and less important in nickel cathodes[85]. Another cycling effect is the structural collapse of the cathode. This effect happens when too many lithium molecules are removed from the cathode, and the molecular structure gets too unstable to support itself. This effect varies with cathode chemistry, and is most present in cathodes with layered structures. In LCO cathodes, only around half of the available lithium molecules can be extracted, before the structural instability leads to rapid loss of capacity[19].

2.8.2 Calendar ageing and Thermal Ageing Mechanisms

The other major factor affecting the lifetime of LIBs is calendar ageing. This is related to the capacity loss of the battery under steady state conditions, which is caused by several different processes. The biggest contributing factor to calendar aging was found to be the temperature of the storage environment and SOC/DOD. Spitthoff *et al.* found that temperature was the largest factor[71]. In general, a battery stored at higher SOC will have a shorter calendar life than one stored a a lower SOC. However, this relation was quite dependent on cathode chemistry, with some being worse than others[71][85].

According to Xiong *et al.*, temperatures either above or below 25 degrees C was found to increase capacity loss. For temperatures below 25C, lithium plating was found to increase, which lead to both capacity loss and loss of safety. For temperatures above 25C, capacity fade increases rapidly the further away from the "comfort zone" of the battery the temperature goes. At higher temperatures, side reactions increase and metal dissolution also increases. The SEI layer thickens and the cathode degrades quicker than at lower temperatures[85].

2.9 Safety Hazards

Some of the most important aspects of LIBs relate to safety. While non ideal temperatures may most of the times result in loss of capacity or higher internal resistance, more extreme temperatures may lead to more serious effects. These cases may result in swelling, heating or even complete destruction of the battery, with potentially catastrophic consequences.

2.9.1 Lithium Plating

During cold temperature operation, typically at temperatures less than 5°C, one of the more serious safety issues is the deposition of metallic lithium on the anode surface. This occurs because of lower diffusivity of the SEI layer and carbon anode[71]. The metallic lithium formation is proportional to temperature and current density, and will start forming moss-like formations and dendrites. These formations may grow into the separator and isolate it from the electrolyte, leading to sudden capacity loss, or it may in rare cases puncture it[2]. This can lead to an internal short circuit, which can lead to thermal runaway.

2.9.2 Thermal Runaway

Thermal runaway is one of the most severe situations that can happen to a LIB. According to Abada *et al.*, the whole process can be described by four distinct stages: At around 90-120°C, depending on cell chemistry, the SEI layer starts to degrade. After the SEI layer has degraded, the electrolyte reacts violently with the now exposed anode active material, which accelerates the increase in temperature. After this step, the the cathode materials start to decompose. This happens at different temperatures depending on chemistry, with the onset temperature being less than 180°C for LCO, over 200°C for NMC, and around 240°C for LFP. When the temperatures have reached above 200 degrees, the electrolyte starts to decompose as well[1]. These reactions will be difficult to stop when they first start, and can lead to the complete destruction of the battery cell with additional damage to the surrounding environment. When the cells are arranged in a pack, the potential for a catastrophic chain reaction also appears, where the thermal runaway of one cell can heat the surrounding cells enough to initiate thermal runaway for those, too.

The reasons for thermal runaway can be numerous, but Feng *et al.* describes how it can be defined into three categories: Electrical abuse, mechanical abuse and thermal abuse. These different types of abuse can affect each other: Mechanical abuse can lead to electrical abuse, which can then lead to thermal abuse. Mechanical abuse can result from collisions or other type of high energy damage. The cells can become crushed by the mechanical forces and tear up the separator, leading to an internal short circuit, or leak electrolyte leading to a fire. In addition, sharp objects may penetrate the outer casing of the battery and lead to the same results. According to Feng *et al.*, this is a more severe failure mode than simple mechanical deformation, but the severity is dependent on the location and size of the penetration[33].

Electrical abuse is another external factor. If the cell is subjected to an external short circuit, the ohmic resistance will generate enough heat to cause a thermal runaway situation[72]. In addition, overcharging and over discharging may also contribute. When the cell is overcharged, lithium plating and dendrite formation is more prevalent and may lead to internal short circuits, as mentioned earlier. When a cell is over discharged, the SEI layer will start to decompose and

generate gases, leading to swelling and a potential thermal runaway situation. However, Feng *et al.* states that more research is required on this subject, and that the safety hazard of over discharge may be underestimated. Thermal abuse may be regarded as the root cause of many different TR situations, as several of the previously mentioned mechanisms result in local overheating of the cell. Thermal abuse may lead to separator shrinking, leading to an internal short circuit. Other, less common issues may be related to loose electrodes and other causes[33].

Overall, the most common root cause for thermal runaway was found to be internal short circuit (ISC)[33]. This is due to the fact that both mechanical, electrical and thermal abuse can lead to it, per the mechanisms previously described. Another type of ISC which is less simple to model and test for is what Feng calls self-induced, or spontaneous ISC. These may result from material contamination or production defects, and may not occur until after days, weeks or even months after initial manufacture. Feng splits the spontaneous ISC into three levels of severity; For level 1, the ISC will not be severe, but can be electrically detected by the BMS due to a slow drop in voltage. For level 2, the voltage drop will be fast, and heat generation will be bigger. The BMS can detect it by a thermo-electrical coupled approach, but the ISC may develop into a full TR event if the heat cannot be dissipated, leading to a level 3 event, where the reactions cannot be stopped, and the cell endures a full thermal runaway with resulting catastrophic consequences[33].

2.10 Comparison of LIB Cathode Chemistries for ESS Applications

An important aspect of designing battery energy storage systems relate to the choice of chemistry. Different chemistries have different performance, cost and safety characteristics, which needs to be taken into consideration when designing and deploying BES systems. Unlike BEVs, specific energy and specific volume is not of the same concern to BESS applications, as the system is stationary and typically doesn't have the same mass and volume constraints as a vehicle does. Additionally, while a BEV used for commuting will typically only endure one charge-discharge cycle per day, a LIB used in ESS applications will tend to have multiple charge-discharge cycles per day[5]. This means that a high cycle life is of a high priority[28]. Lastly, while safety is important for all LIB applications, large scale grid storage systems can have capacities of several hundred megawatt-hours and are critical pieces of electrical infrastructure, which means that a potential thermal runaway situation could have serious consequences[23]. This section will therefore compare the NMC, NCA and LFP chemistries in the relevant categories of cycle life, cost and thermal safety.

2.10.1 Cycle life

In a report by Yuliya Preger *et al.*, the cycle life of commercial NMC, LFP and NCA cells was examined by cycling the cells under different conditions. The performance of the different cells was then compared to previous studies. The cells were subjected to temperatures of 15, 25 and 35 degrees C, as well as C-rates from 1 to 3, except for the NCA cell, where the C-rate of 3 was outside manufacturer specifications. The Equivalent Full Cycles (EFC) to reach 80 % of initial capacity was found. The authors found that LFP was had the highest cycle lifetime in all conditions, which was also consistent with other results by Keil (2016) and Sandia (2019)[50][65]. The report also showed that LFP was less affected by DOD compared to NCA and NMC. At 25 degrees C and 0.5C discharge rate, the LFP cells had over 90 % capacity retention after 3000 equivalent full cycles, while the NMC would reach 80 % capacity after less than 2000 cycles, depending on DOD value.

With full 0-100 % DOD, the NMC cells could not reach 500 cycles until degrading below 80 %. The NCA cells could reach over 1500 cycles until reaching 80 %, but only at 40-60 % DOD[65].

2.10.2 Cost

Cost is undoubtedly an important consideration in BESS design and deployment. While the deployment cost of energy storage system can vary, this thesis will concentrate on the cost of the battery cells themselves, as that gives the clearest basis for comparison between the cathode chemistries. Giving an accurate cost comparison between popular cathode chemistries can be challenging, as the actual cost of cells varies greatly, depending on many different factors, like raw materials prices, production capacity and supply chain issues. Some older studies, like one by Patry *et al.* from 2015, modelled the cost of NMC, LFP and NCA cells, and discovered that NMC was the most cost-effective at 233 dollars per kWh, while LFP was the most expensive at 285 dollars[62]. However, while this model may have been accurate in 2015, the cost of LIBs have dropped greatly since then.

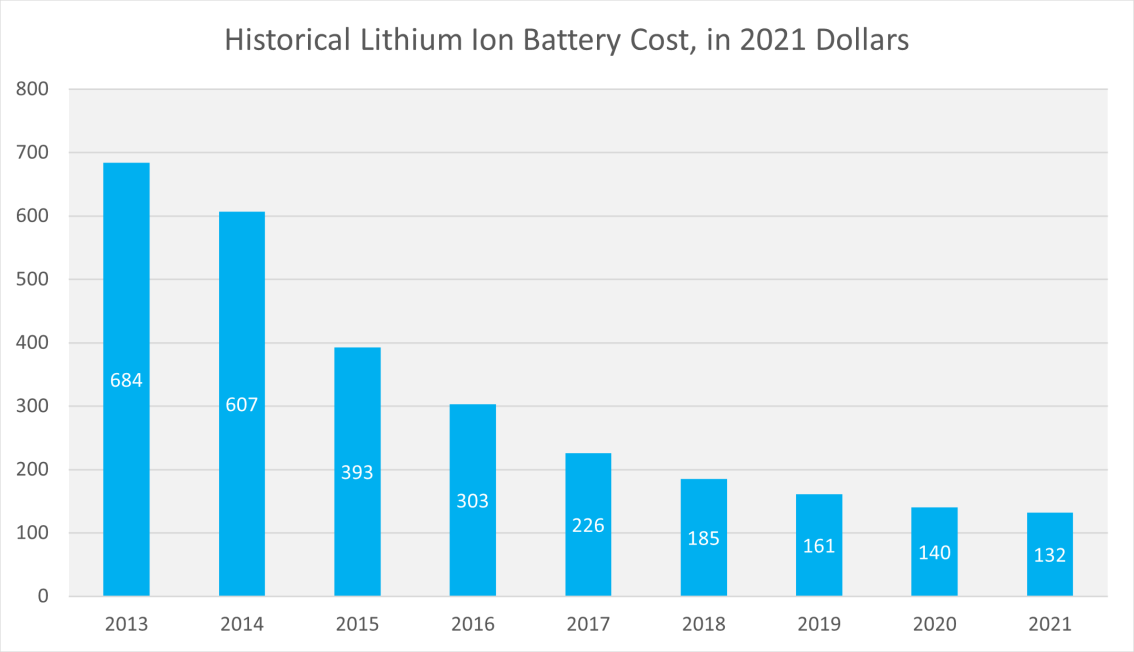

Figure 14: Cost comparison of LIB packs since 2013. Data provided by BloombergNEF[41].

According to BloombergNEF, battery pack prices have fallen 89 % between 2010 and 2021, to 132 dollars per kWh in 2021. The historical cost split between cell and pack is shown in Figure 14. The development shows that pack cost is lowering in relation to cell cost, and that the total cost of battery packs is has lowered dramatically. The cost decrease was primarily driven by low LFP cell prices, which were on average 30 % cheaper than NMC cells. The relatively high cost of NMC was cited to be due to high cobalt prices, which doesn't influence LFP. However, LFP was also found to be vulnerable to high lithium carbonate prices. In general though, LFP was still found to be the cheapest type of LIB compared to its peers[41].

Table 2.1. ARC results from Brand *et al.*			
	Type	T_{onset}	T when rate >5°C/min
1	LFP	104°C	287°C
2	LFP	81°C	212°C
3	NMC	88°C	212°C
4	NCA	86.5°C	183°C

Table 2.1: ARC results from Brand *et al.* [16]

2.10.3 Thermal Safety

There are differences in the thermal safety between different LIB cathode chemistries. Brand *et al.* conducted accelerated rate calimetry(ARC) tests on NMC, LFP and NCA pouch cells. This test was used to detect self heating after the battery was heated up. The tests showed that LFP needed to be heated up the most before reaching a rate of temperature increase of >5 degrees per minute. NMC was second, and NCA was the worst in this regard[16]. See table 2.1 for more specific results. The report further elaborated that LFP had significantly higher thermal stability than both NMC and NCA, which both reached temperature rates of over 400C/minute, compared to just 28deg C/minute for the LFP cell[16]. This is due to the olivine structure of the LFP cathode, which won't have an exothermic decomposition reaction causing the electrode to release oxygen to then react with the electrolyte[60][68].

3 Methods

3.1 Goals

The main goal of this thesis was to estimate the resource and energy requirements of a large scale, global adoption of lithium ion battery energy storage systems (LIB ESS). Four requirements were going to be analysed:

A. The required global installed LIB ESS capacity to satisfy the VRE penetration of NZE, APS and STEPS.

B. The inflow and outflow of LIB ESS to sustain the required installed capacity.

C. The raw material required to sustain the estimated inflow and outflow values.

D. The greenhouse gas emissions of manufacturing the required amount of LIB ESS.

In order to achieve these goals, a spreadsheet model was developed in Microsoft Office Excel, named the Battery Energy Storage Estimated Requirement Model (BESSER). The main components of BESSER are described in the following sections.

3.2 Standardised Battery Energy Storage System

In order to estimate material and resource requirements for a battery pack, the precise material contents for a battery of a given energy capacity (and its associated systems) is needed. While in real life, the deployment of BESS can be achieved by several different types of systems. The variety of these systems made estimating the potential resource use challenging. Because of this problem, the analysis was designed around a Standardised Containerised Energy Storage System (SCESS). By having a standardised ESS installation, calculating the resource use became significantly less challenging. The system was based on real container-based BES systems.

Overall SCESS design: The SCESS was designed around the standard 40 foot ISO intermodal container, in a similar fashion to several commercially available systems. The system consisted of 24 separate, self contained battery packs, each one lined up against the inside walls of the container in rows of 12 individual packs (24 in total). In the space between the packs, there is an aisle for access to each pack. The internal layout is illustrated in Figure 15. The battery packs were designed by using BatPaC, an Excel based battery manufacturing and cost estimation model made by the Argonne National Laboratory (ANL). More specifically, the model used was BatPaC V2 Beta. This was acquired through the US Environmental Protection Agency (EPA)'s website[9]. This specific version was from 2011 and could be regarded as outdated by today's standards, but was the only one publicly available to the author in the time period of which it was acquired. BatPac V2 was specifically designed for batteries used in BEVs, PHEVs and HEVs, with no explicit stationary battery designs available. The battery designed for this thesis was therefore an approximation based on BatPaC V2's built in battery design.

Thermal Management System: BatPac gives the user a choice between liquid cooling and air cooling as forms of thermal management systems (TMS). For the SCESS design, BatPac's liquid

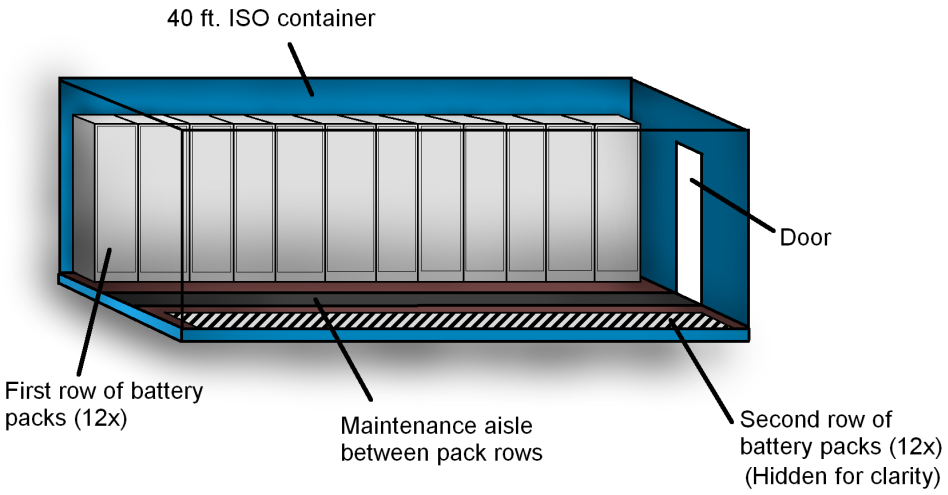

Figure 15: Internal layout of the Standardised Containerised Storage System (SCESS).

cooled design was chosen. While this design choice affects the performance parameters of a real life BESS, for an analysis focusing on material, energy and resource use, this option is less relevant. However, liquid cooling was still chosen, as it is the best performing TMS for a given application. For the SCESS design, the wider components of the TMS (heat pumps, air conditioning systems, et cetera) were not included, as this was regarded as less relevant for the wider analysis, especially when taking the large variety of different available systems into account. Additionally, mass and volume the working fluid of the liquid TMS was not considered relevant for the further material analysis, and was included.

Battery chemistry and other parameters: For this analysis, lithium iron phosphate ($LiFePo_4$, LFP) was selected as the cathode chemistry. Graphite was chosen as anode chemistry. The reason for choosing LFP was mainly due to the fact that it's quickly becoming the preferred chemistry for BESS, and it was assumed that this specific chemistry will dominate the future market too. The analysis therefore assumed that the future expansion of the BESS market will mainly be centred around LFP chemistry. With chemistry now established, the "chemistry"-section of the BatPac spreadsheet was changed to "LFP-G". Further, in the "Battery Design" section, inputs were added, as shown in the table (Battery design). This allowed the full SCESS to have an energy capacity of 2400 kWh, which is a realistic value for similar real life systems, as well as not exceeding the weight limits of the intermodal container nor the internal volume restrictions. The values resulting from the BatPac simulation were subsequently added to the main spreadsheet on which the main analysis was based to be used for calculating material and resource use.

3.3 Required future energy storage capacity

In order to estimate the resource and energy requirements of the future battery energy storage sector, it was imperative to know the future demand of battery storage. The first step of the analysis was therefore to estimate the future required battery energy storage capacity. The basis of the analysis was the VRE penetration and energy demand from the International Energy Agency's

Material Summary for SCESS		
Material	Weight (kg)	Weight per kWh
Lithium	212.99	0.09
Iron	1714.05	0.71
Phosphorous	950.48	0.40
Carbon	2998.50	1.25
PVDF	412.61	0.17
$LiPF_6$	2.16	0.00
Copper	254.21	0.11
Aluminium	3803.04	1.58
Steel	3750	1.56

Table 3.1: Summary of the weight of each material in one SCESS system, as well as the weight per kWh of battery. The carbon entry counts both for the graphite anode material and carbon black. Data from BatPaC-V2.

Net Zero by 2050 Scenario, Announced Pledges Scenario and Stated Policies Scenario scenario.

The goal of the analysis' first step was to calculate the future energy capacity of global battery energy storage systems (BESS). This was achieved by correlating each scenario's share of variable renewable energy penetration with the fraction of energy demand required by storage, as discussed in the Theory section. In this case, the 2050 values for VRE penetration were 68 %, 52 % and 40 % for NZE, APS and STEPS respectively. For this, the analysis is bases itself on the findings of Zsiborács *et al.* in their report on the role of Energy Storage in Europe in 2040[89]. Their research created a polynomial regression model which was based on seven different studies. The regression model indicated the required energy storage fraction (energy storage/energy demand per year) and how it correlated with a specific percentage of VRE penetration in the European market. It's important to stress that their model was an estimate for a relatively localised geographical area (Europe), and that for a global market, which is what this thesis is assessing, the results would likely be different. Due to difficulty using the original equation in a spreadsheet model, the report's resulting data points were inserted into a spreadsheet, where Excel's solver tool was applied to a modified logistic function to obtain a workable equation with similar results to the original.

In order to obtain the required energy storage requirement for future energy mixes, the energy storage fraction was applied to the future levels of VRE penetration and electricity demand. This data was obtained from the earlier mentioned IEA scenarios, with the first scenario to be modelled being NZE. The years included in the model were 2020 to 2050. For each of the three chosen IEA scenarios, the VRE penetration and electricity production were inserted into the spreadsheet. In the IEA-sourced spreadsheets, only the values from 2020, 2030, 2040 and 2050 were available, so the Excel Solver tool was used to create non linear regression models based on sigmoid functions. In this way all the relevant values for each individual year from 2020 to 2050 could obtained.

When the VRE penetration, energy production and storage fraction were obtained, they were inserted into the spreadsheet model. By multiplying the calculated storage fraction from with the energy production of each consecutive year, an estimate in TWh for the total installed ESS capacity for each year from 2020 until 2050 was obtained. This estimate was a cumulative number of the required installed capacity for each years VRE without considerations towards storage technology or replacements - it was simply an indicative value of how much energy storage is needed for future energy production and VRE penetration.

There was great uncertainty regarding the share of future ESS energy capacity covered by batteries.

There have been several studies covering the future technology mix of the energy storage market, with the technology mix varying between studies. In a paper by Alhelou *et al.*, the effects of different energy storage technologies were explored in context with using electric vehicles as energy storage. In the paper, the power grid of Spain was modelled with high wind power penetration. For the Spanish grid modelled, the storage technologies used were CAES, EV vehicle to grid, PHS and LIB ESS. The paper evaluated combinations of the different storage technologies, with the scenario combining GMD, DR, ST and EVs demanding the least energy storage, while the scenario only using GMD and ST demanding the most. However, the energy capacity share of BESS in relations to the other storage technologies was relatively constant, ranging from 16.2 % to 22.9 %[5]. In all three scenarios, CAES dominated the storage capacity. Therefore, as a benchmark for a potential future storage technology mix, this thesis chose to set the technology mix for the BESS at 20 % of the total ESS storage capacity demand. By multiplying this value with the already determined future ESS demand, the required BESS capacities for each IEA scenario was obtained. In order to find the annual installation rate of BESS in TWh/year, the inflow value was calculated, taking the cumulative BESS energy capacity (from the previous section) and subtracting the value for each year with the value for the previous year.

3.4 Inflow/Outflow Modeling

In order to estimate the true requirements of future BESS deployment though, it was not enough to simply know the required amount of BESS energy capacity in relations to the previous factors, as those calculations did not take battery ageing and failure into account. As such, the true resource requirements of large scale BESS deployments are going to be higher than the initial calculations, as the batteries fail over time and have to be replaced by new units. For this analysis, a cumulative failure Weibull distribution was used to model battery pack failure rates. The failures were binary, i.e a battery was regarded as either functioning or completely failed. This meant that the effects of battery degradation in terms of capacity fade and other adverse effects of age were not taken into account, as these would have resulted in a significantly more complex model, which was out of scope for this analysis.

The Weibull distribution for this analysis was used for modelling the cumulative cell wear out failures. The cumulative Weibull equation uses two main parameters, the shape parameter α, and the characteristic life β. t is the time in years from the batteries were installed, and *F(t)* is the percentage of batteries that have failed after a given amount of years.

$$F(t) = 1 - exp(-(t/\alpha)^{\beta}) \tag{1}$$

For this analysis, β was set to be 10 years and α was set to 5. While the time before failure of BES systems vary, a characteristic life of 10 years was regarded as a realistic value for this analysis, as the same value was used by Zubi *et al.* when describing the average time until battery return for ESS[90]. In a Weibull distribution, a characteristic life of 10 years means that 63.2 % of failures will happen after 10 years. As the failure distribution was cumulative, the failure rate was calculated for each respective year in the spreadsheet model by multiplying the cumulative failure distribution with each respective inflow value. This resulted in an outflow value of a certain TWh/year, which was estimated from the previously calculated inflow value. In order to then accurately compensate for the lost capacity that the outflow caused, a compensated inflow value was obtained by adding

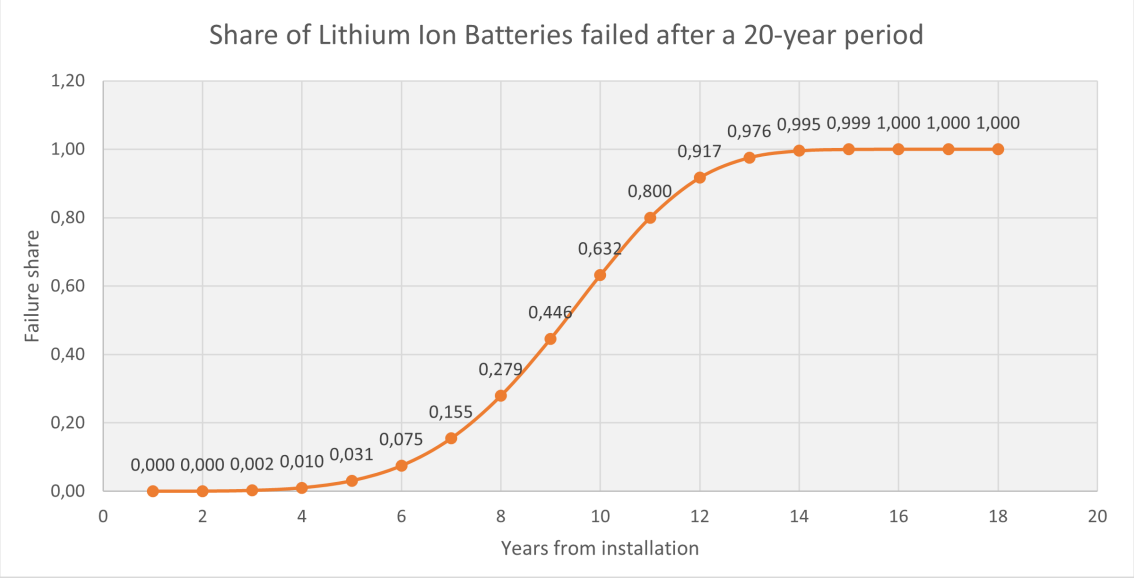

Figure 16: The share of installed batteries which fail over a 20 year period. Modeled on a cumulative Weibull distribution, shape parameter 5 and characteristic life 12 (years).

the outflow value from the inflow value for each subsequent year. This resulted in an inflow and outflow rate of BES systems for each year in each separate scenario which would be used to more accurately model the requirements of the previously established future BESS demand.

3.5 Material Requirements

In order to calculate the material requirements for the three scenarios, the material contents for a given energy capacity of LIB had to be obtained. For this thesis, the following materials were analysed. Lithium (Li), Iron (Fe), Phosphorous (P), Carbon (G), Polyvinylidene fluoride (PVDF), Lithium hexafluorophosphate ($LiPF_6$), Copper (Cu) Aluminium (Al), and Steel (S). Of these, Li, Fe and PO4 were the cathode active material, carbon in the form of graphite was the anode active material, PVDF is the binder used in the anode and cathode and $LiPF_6$ is the electrolyte. Copper foil is used as the conducting material in the anode, and aluminium is used for the same purpose in the cathode. Additionally, aluminium is used as the structural material for the battery pack itself. Steel is mainly used in the intermodal 40 feet container.

By using the SCESS model, the material mass for each individual SCESS of 2400 kWh was calculated by using values from BatPaC. From this outset, it was trivial to obtain the same values per kWh. The material resources contained in the SCESS were then categorised in two sections: Annual Material Inflow and Annual Material Outflow. Each of the previously discussed materials were then inserted into these sections in terms of kg/Twh and multiplied with the corresponding battery inflow/outflow value (TWh/year) from the Inflow/Outflow section. By doing this, the material requirements for each year in each scenario were obtained.

3.6 Greenhouse Gas Emissions

For estimating the greenhouse gas (GHG) emissions of the future BESS demand, the LIB production GHG emissions per functional unit (TWh) needed to be obtained. Previously desribed studies

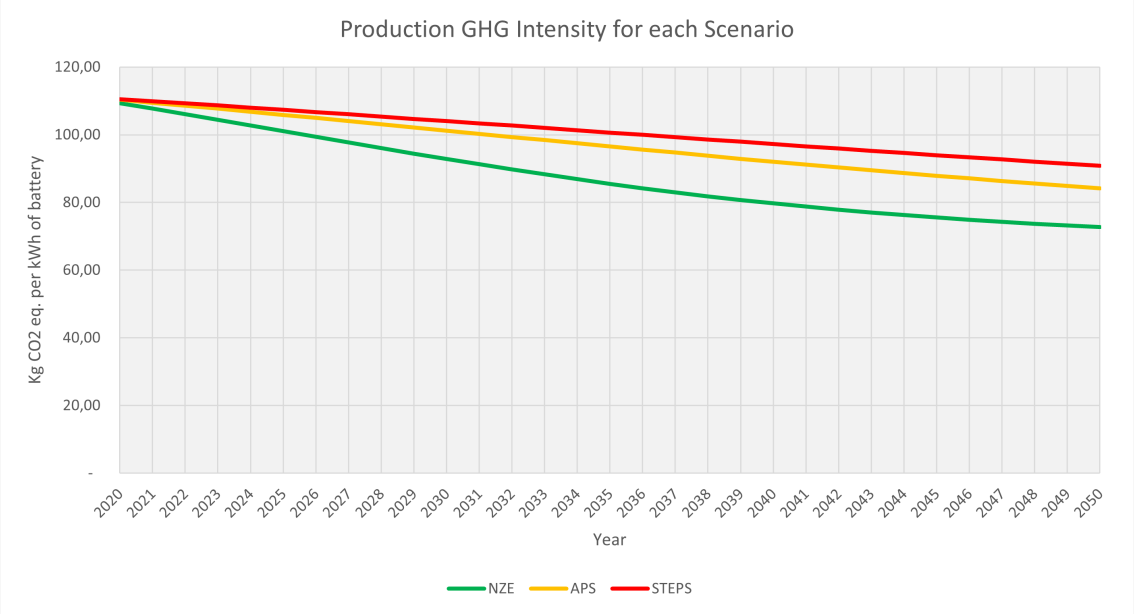

Figure 17: Greenhouse Gas emission intensity for producing 1 kWh of LIBs.

were scrutinised by the author to find a value which would give a realistic picture of GHG emissions from large scale LIB production with a LFP chemistry. A particular challenge was the great differences in emission magnitude between the different studies, with the total span of emissions ranging from 38 to 356 kg CO_2 Eq/kWh. After consultation between with supervisors, an initial value of 110 kg CO_2 Eq per kWh of battery was used. This is a similar value to the emission intensity obtained by Hao *et al*[38]. It is also inside the middle of the range of Emilssons report[32]. A GHG value of 110 is lower than the LFP-focused LCAs studied by Ellingsen (the lowest was 150), but those studies were from 2010-2013. The author of this report therefore deemed it plausible that the GHG emissions are of a lower magnitude with modern production processes, especially in regards to improvements in cell production and cathode material production processes.

Another effect which was included in the GHG emission estimation was the transition towards renewable energy (RE) and its impact on LIB production emissions. The results from Hao *et al*, Emilsson and Ellingsen were taken into consideration when determining the potential emission reductions from RE adoption, and a emission reduction of 50 % was determined to be reasonable. The renewable energy shares from the three IEA scenarios in the years 2020, 2030 and 2050 were adapted into the BESSER spreadsheet by utilising the Excel Solver tool and the SSR method. An equation for estimating the reduction of GHG emissions in LIB production was obtained, which took the scenario-wise RE share into account. This equation was then applied to the initial GHG emissions in each scenario. The resulting emission intensity (In kg CO_2 Eq/kWh of battery produced) is displayed in Figure 17. The emission intensity values for each year and each sceario were then applied to the inflow and outflow values which were already calculated for each scenario, to find the resulting LIB production GHG emissions for each year and IEA scenario.

4 Results

In order to produce an estimate of future requirements for battery energy storage deployment, the parameters discussed in the 'Methods'-section were loaded into the BESSER spreadsheet model. The requirements for future LIB BESS installed capacity, inflows and outflows due to battery EOL, raw material requirements, and production phase greenhouse gas emissions were calculated for each of the respective IEA scenario studied in this report. The final results are shown in this section.

4.1 Required LIB Capacities for each IEA Scenario

The first results to be discussed is the requirement for BESS energy storage capacity for each respective IEA scenario. The values, graphed for each year until 2050, are shown shown in Figure 18. The figure shows the required installed BESS capacity, based on equation (1) and the IEA scenario values for energy production and VRE penetration. These results do not take into account any in- or outflows of energy capacity, they only show the required installed BESS capacity for a given year for each scenario.

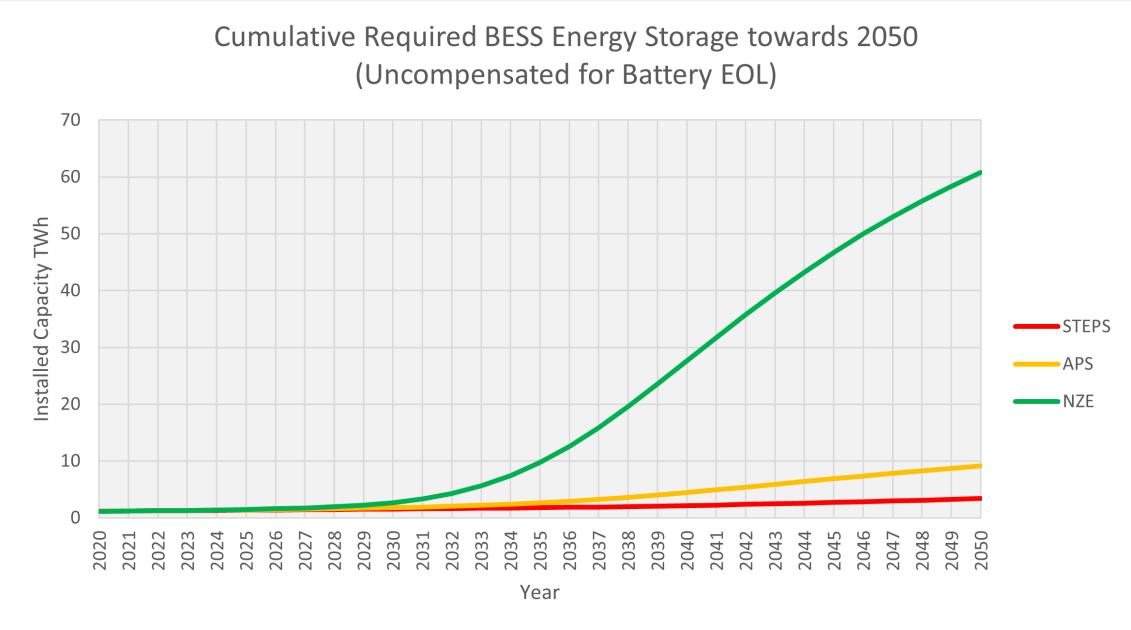

Figure 18: The requirement of installed BESS capacity for each IEA scenario, based on the VRE penetration and electrical energy demand, as well as technology mix of 20 % LIB storage. The in- and outflows of battery capacity due to degradation is not taken into account in this graph.

The results show a relatively low demand for BESS capacity for all three scenarios from 2020 towards 2030, where the model shows the beginnings of a sharp increase in storage requirement for the NZE scenario. For this scenario, the slope increases until around 2038, continuing to increase relatively steadily until 2050, ending at a final value of 60.76 TWh of installed capacity. For the APS scenario, the increase instead rises relatively slowly, but with a marked increase at around 2035, continuing to rise at a relatively stable rate until 2050, ending at an installed capacity of 9.13 TWh of installed capacity. For the STEPS scenario, the rise is relatively stable during the entire period, ending at an installed capacity of 3.39 TWh of installed capacity. A significant

disparity is observed between the required capacity of each scenario, most notably between the NZE scenario and the others. The installed BESS capacity for NZE in 2050 is caclulated to be 6.655 times higher than for APS, and 17.923 times higher than STEPS. A common factor between the scenarios is a sharp increase in required capacity in the decade from 2030 and onwards. Still, the scenario-wise differences are significant; The storage requirement of APS in 2050 is similar to the storage requirement of NZE as early as 2035.

4.2 Inflow/Outflow due to LIB End of Life

The next line of results from BESSER were the battery inflow and outflow estimations for each scenario. The failure rate was calculated by using a Weibull estimation with the shape parameter of 5 and a characteristic life of 10 years. The values for the in-and outflow of battery capacity is based on the cumulative required installed capacity shown in Figure 18, combined with the failure rate from the Weibull distribution. The resulting graphs show the inflow and outflow of battery capacity, in TWh/year, for the years toward 2050.

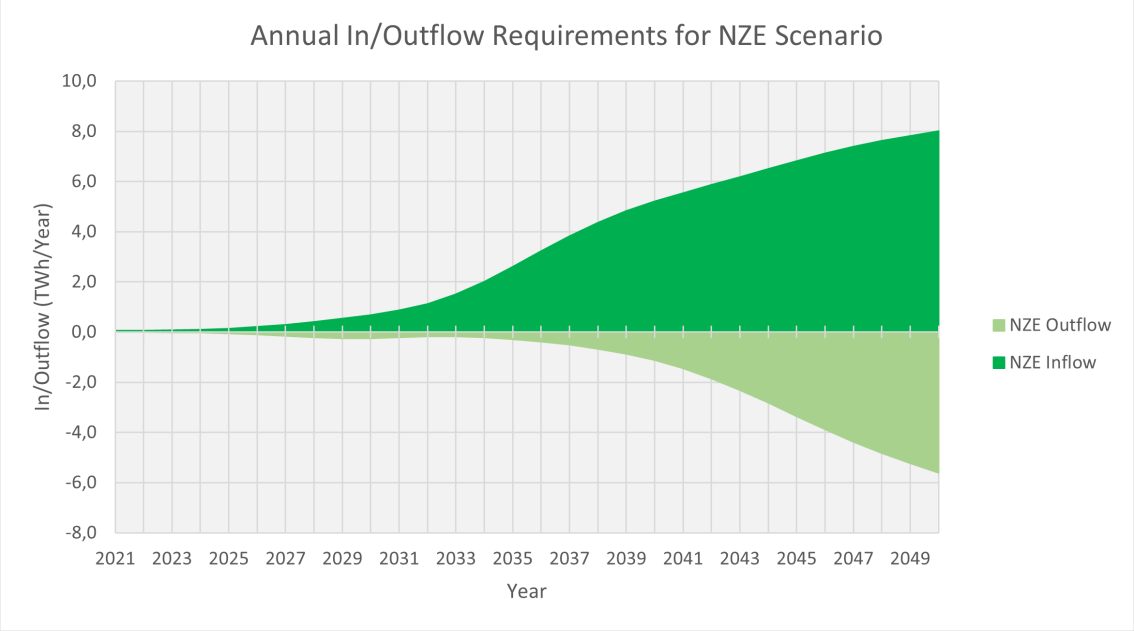

Figure 19: The inflow and outflow of battery capacity caused by LIB degradation for the NZE Scenario.

For the NZE scenario, displayed in Figure 19, the in- and outflow analysis show a marked increase of capacity inflow around 2030, with a value of 1 TWh/year passed in 2032. The increase has a slight stabilisation around 2039, continuing with a linear increase towards 2050, peaking at 8.01 TWh/year in 2050. For the outflow, the values start to increase around 2026, showing a local maximum of 0.246 TWh/year in 2030 as the capacity installed in the 2020s start to degrade and reach end of life in larger numbers. This decrease in installed capacity does affect the inflow values accordingly, but the effect is not noticeable in the graph due to the inflow being dominated by new installations to satisfy the growing need for BESS in the NZE scenario. The outflow starts to increase again in 2036 and grows steadily towards 2050, peaking at 5.61 TWh/year.

For the APS scenario, displayed in Figure 20, the in- and outflow analysis show an increase in outflow from the mid 2020s and a local maximum of 0.243 TWh/year in 2029. A corresponding

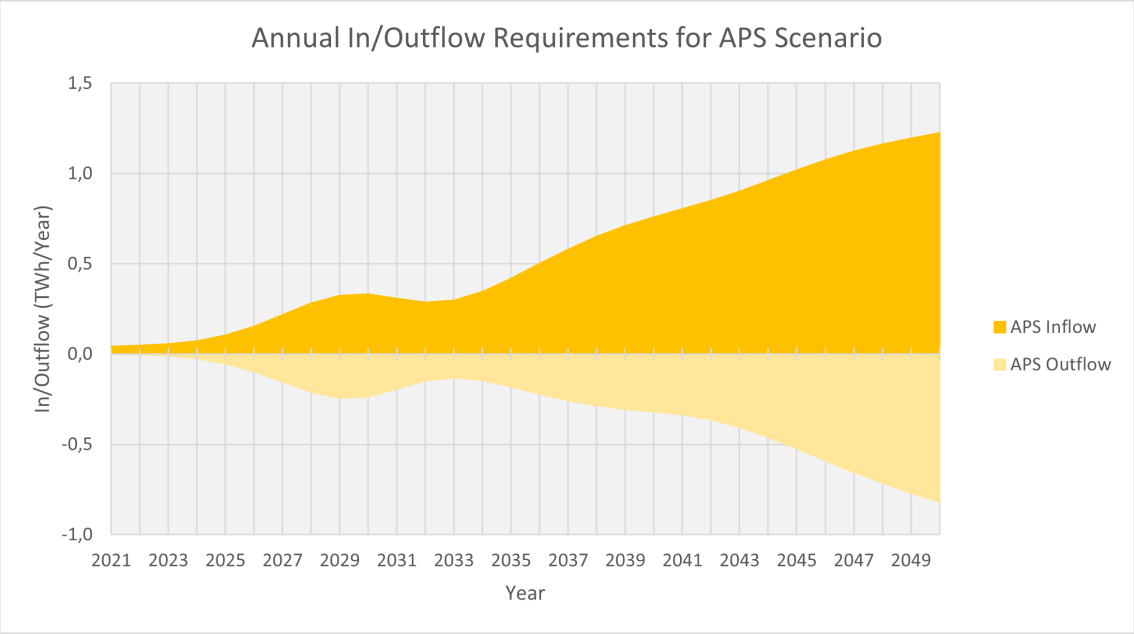

Figure 20: The inflow and outflow of battery capacity caused by LIB degradation for the APS Scenario.

increase in inflow is observed in the same period, but with an inflow rate of over 0.332 TWh/year in 2030. A new increase in outflow is observed from 2034, rising relatively linearly until 2042, then showing an increase, and peaking at 0.821 TWh/year. A similar pattern is observed in the inflow values, but the increase is relatively linear before reaching a peak of 1.225 TWh/year in 2050. In summary, the APS Scenario displays two distinct periods of high required inflow; The first arrives in the mid to late 2020's, mostly due to the replacement of degraded battery systems installed in the early 2020's. The inflow then stays relatively stable until the second increase arrives in the early to mid 2030's, when the demand for battery installations increases, combining with the systems installed during the 2030s starting to degrade and needing replacement.

For the final WEO scenario, STEPS, the results are displayed in Figure 21. In general, the results show a similar pattern to APS, althogh the magnitude of the inflow and outflow values is significantly lower. In a similar fashion to APS, a local maximum is observed in the in/outflow values around 2029, combined with a lowering in installation rate, and then an increase after 2033. In the first local maximum, the values for inflow and outflow are 0.280 and 0.241 TWh/year respectively. The APS scenario is characterised by an overall significantly lower required installed BESS capacity than the other WEO scenarios, peaking at an inflow value of 0.463 TWh/year in 2050. This results in lower inflow and outflow values in the last two decades of the scenario, but the values are more affected by the degradation replacements in comparison to the other two scenarios.

The results of all three scenarios are displayed in Figure 22. In summary, the in/outflow analysis revealed great differences between the three IEA scenarios, and some distinct similarities. In a similar way to the storage requirement analysis, the NZE scenario is by far the most intensive in terms of both inflow and outflows, peaking at 8.01 and 5.61 TWh/year respectively, which is 6.54 times as much as the APS scenario. For NZE, a cumulative inflow value of 102.13 TWh is needed over a 30 year period, while APS and STEPS need 17.97 and 8.78 TWh respectively.

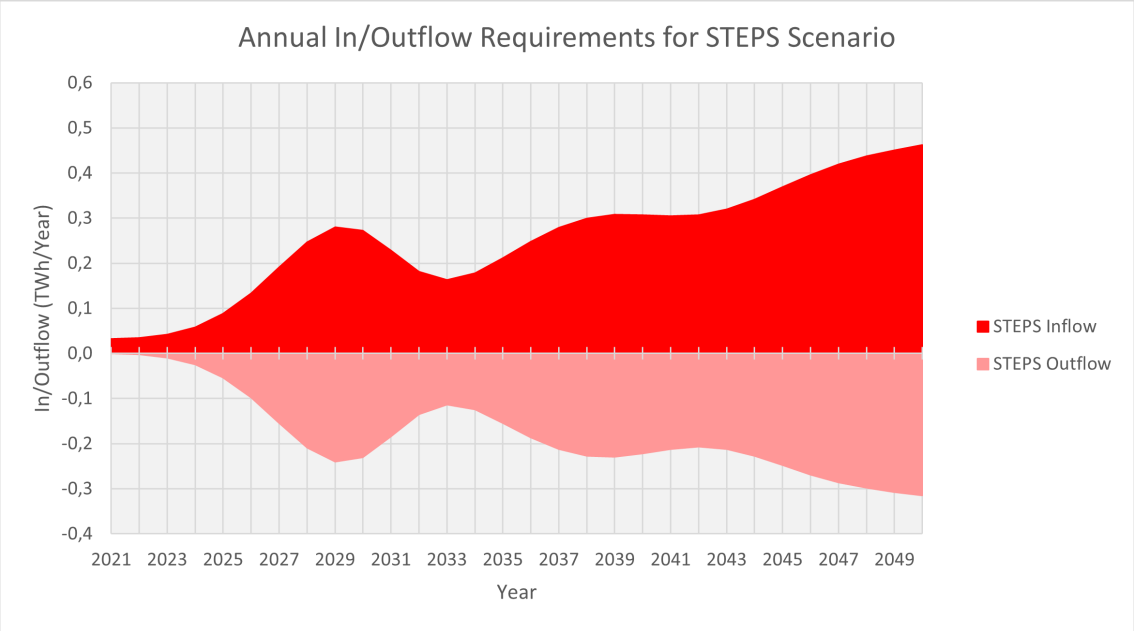

Figure 21: The inflow and outflow of battery capacity caused by LIB degradation for the STEPS Scenario.

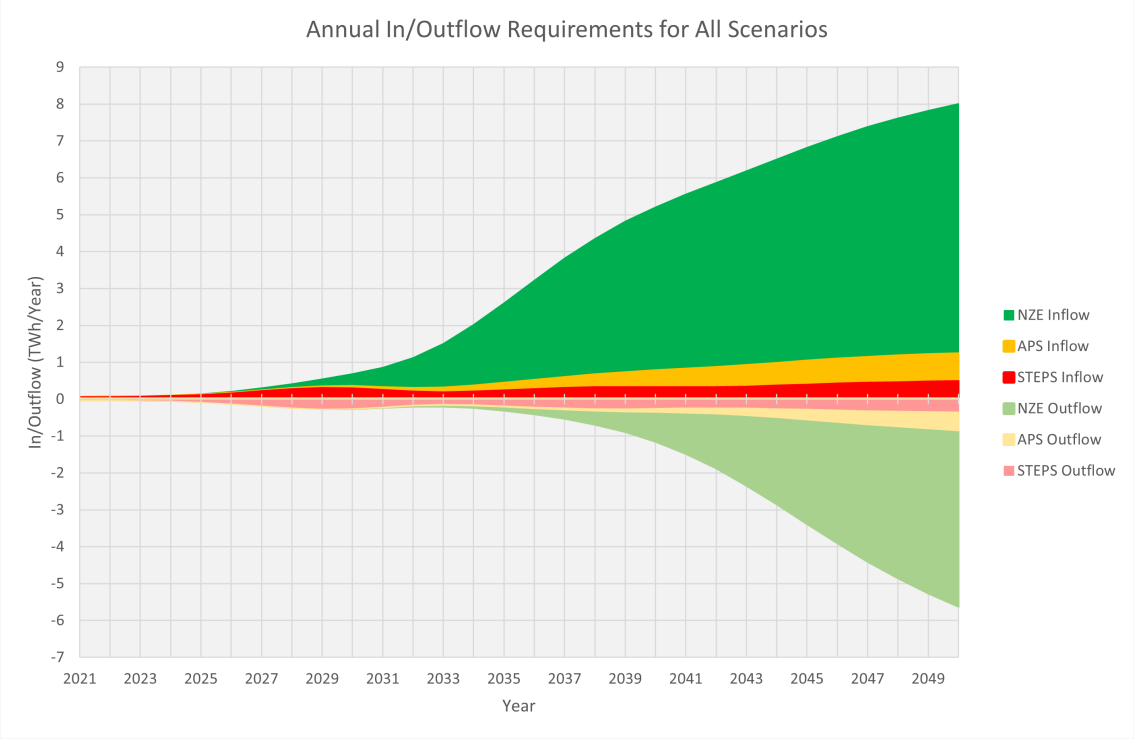

Figure 22: The inflow and outflow of battery capacity caused by LIB degradation for all scenarios, superimposed on each other to show differences in scale. The colour coding is still present.

4.3 Raw Material Requirements

The next results calculated in BESSER was the raw material requirements. These values were calculated by using the material weight percentage from the SCESS design and the inflow and outflow values from the in/outflow analysis. The resulting values were the annual material inflow

and outflow requirements, in tonnes per year. The values are shown in Tables 4.1 to 4.3.

Material inflow requirements for the NZE Scenario, in tonnes/year				
Material	2021	2030	2040	2050
Lithium	5 171	60 484	462 085	710 755
Iron	41 615	486 747	3 718 650	5 719 838
Phosphorous	23 077	269 911	2 062 070	3 171 770
Carbon	72 800	851 497	6 505 270	10 006 075
PVDF	10 018	117 170	895 156	1 376 883
$LiPF_6$	52	612	4 676	7 192
Copper	6 172	72 188	551 506	848 298
Aluminium	92 333	1 079 965	8 250 720	12 690 836
Steel	91 046	1 064 903	8 135 649	12 513 840

Table 4.1: Material inflow requirements for the NZE Scenario for the years 2021, 2030, 2040 and 2050.

Material inflow requirements for the APS Scenario, in tonnes/year				
Material	2021	2030	2040	2050
Lithium	3 842	29 424	67 348	108 694
Iron	30 920	236 793	541 990	874 717
Phosphorous	17 146	131 307	300 545	485 049
Carbon	54 090	414 238	948 137	1 530 199
PVDF	7 443	57 001	130 468	210 563
$LiPF_6$	39	298	682	1 100
Copper	4 586	35 118	80 381	129 728
Aluminium	68 603	525 383	1 202 534	1 940 771
Steel	67 647	518 056	1 185 763	1 913 704

Table 4.2: Material inflow requirements for the APS Scenario for the years 2021, 2030, 2040 and 2050.

Material inflow requirements for the STEPS Scenario, in tonnes/year				
Material	2021	2030	2040	2050
Lithium	2 840	24 139	27 261	41 051
Iron	22 857	194 257	219 386	330 364
Phosphorous	12 675	107 720	121 654	183 194
Carbon	39 986	339 827	383 787	577 926
PVDF	5 502	39 083	52 811	79 525
$LiPF_6$	29	244	276	415
Copper	3 390	28 810	32 537	48 996
Aluminium	50 715	431 007	486 762	732 991
Steel	50 007	424 996	479 973	722 768

Table 4.3: Material inflow requirements for the STEPS Scenario for the years 2021, 2030, 2040 and 2050.

For the NZE Scenario, the resulting material inflow values are displayed in Table 4.1. Of particular interest are the values for lithium and phosphorous. The table shows a 2050 demand of over 700 000 tonnes of lithium per year, and over 3.1 million tonnes/year of phosphorous, which is 7.2 million tonnes when converted to the phosphate rock (P2O5) definition used by the USGS[77]. The results show a significant increase in the material inflow requirements over the 30 year period of the scenario, with the largest increase happening in the decade from 2030 to 2040. For the APS

Cumulative Material Requirements, in metric tonnes			
Material	NZE	APS	STEPS
Lithium	9 063 421	1 595 080	779 035
Iron	72 938 338	12 836 487	6 269 325
Phosphorous	40 445 843	7 118 102	3 476 472
Carbon	127 595 657	22 455 679	10 967 327
PVDF	17 557 761	3 090 007	1 509 156
$LiPF_6$	91 714	16 141	7 883
Copper	10 817 346	1 903 755	929 792
Aluminium	161 831 249	28 480 833	13 910 005
Steel	159 574 231	28 083 619	13 716 006

Table 4.4: The Cumulative Material Requirements towards 2050 for all scenarios.

scenario, a similar trend can be observed, but the increase from 2030 is less dramatic, and ends with a significantly lower material inflow value in 2050, at over 91 000 tonnes per year in the case of lithium. For the STEPS scenario however, the largest increase in material inflow occurs from 2020 to 2030, but the increase from 2030 to 2050 is less than for the first decade. As with the other results, large differences between the scenarios are observed, with the NZE scenario having a significantly higher demand for materials than either APS and STEPS. As the values are calculated on a tonne per TWh basis, using the capacity in- and outflow analysis from the previous section, results for material inflow and outflow correlate directly with the results from Figure 18. The cumulative material requirements (in tonnes) are displayed in Table 4.4.

4.4 Greenhouse Gas Emissions

The final result to be calculated was the LIB production GHG emissions of each scenario. This was obtained by using the GHG estimation from the BESSER spreadsheet. The resulting values were the GHG emission rate, in tonnes of CO_2 equivalents per year. This is shown in Figure 23. The results show a 2030 emission rate of less than 30 million tonnes of CO_2 for APS and STEPS, while the NZE scenario sharply increases its emission rate. This increase continues until the end of the scenario, but with a noticeably lower steepness from around 2040, increasing with a relatively linear rate, peaking at 582 419 tonnes/year in 2050. The APS scenario shows significantly lower emission rates than the NZE scenario, and appears to almost stabilise after 2044, ending at a final value of 103 066 048 tonnes/year. This is just 17.5 % of the final NZE value. For the APS scenario, the values show an initial local maximum corresponding to the increase in new LIB installations in the late 2020s, then a decrease and subsequent increase from 2037. The final emissions stabilise from the early 2040s to end with an emission rate of 42 011 117 tonnes/year in 2050.

The cumulative values of GHG emissions were 872 992 999, 1 660 546 611 and 8 011 899 665 tonnes of CO_2 equivalents for the STEPS, APS and NZE scenario respectively. In broad terms, the differences between the scenarios mirror the in/outflow values, but they are also impacted by the lowering emission rate of LIB production as a consequence of higher shares of renewable energy.

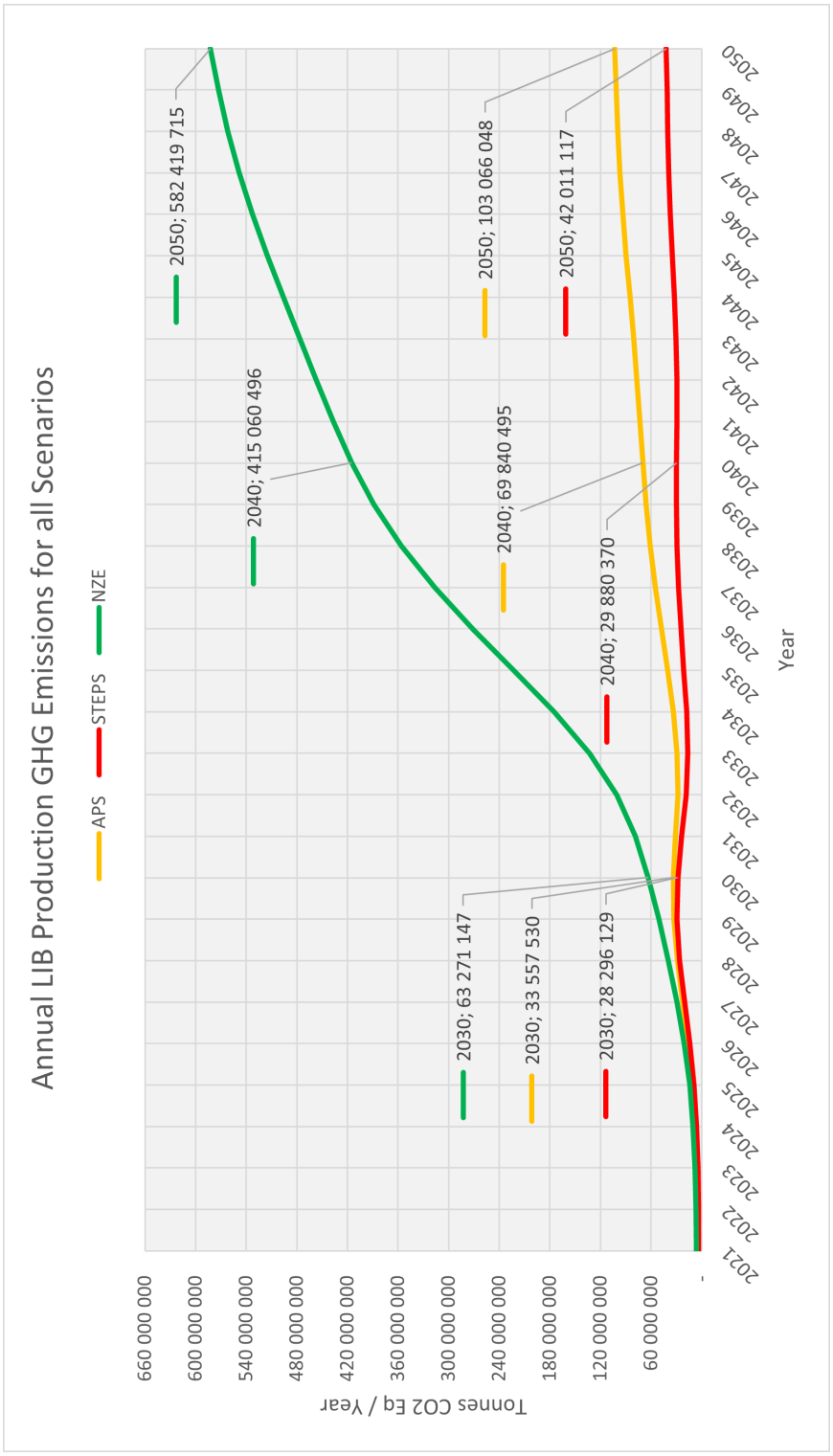

Figure 23: The production phase greenhouse gas emission rate for each scenario, in tonnes of CO_2-equivalents per year.

5 Discussion

The results of the scenario-wise analysis of large scale LIB ESS deployment showed significant differences between each of the IEA scenarios, in all surveyed categories. The NZE scenario is a significant outlier in the analysis, as it required almost 18 times as much installed capacity in 2050 than the STEPS scenario, while it required 6.5 times as much installed capacity than the APS scenario. For comparison, the APS scenario required only 2.69 times as much required storage capacity than STEPS. While obviously not matching the exact values, the significantly larger requirements of the NZE scenario were observed in the Inflow and outflow analysis, material analysis and the GHG emission analysis.

5.1 Influence of VRE Penetration on Storage Capacity

There were several reasons that the analysis generated large observed differences. The most significant reason is the share of VRE generation in each of the IEA scenarios. STEPS had a 2050 VRE penetration of 40 %, APS had 52 %, and NZE had 68 %. This difference was exacerbated when the energy storage fraction was calculated in equation VRE, as the relationship between the storage fraction and VRE penetration could be described as almost exponential. This relationship was described by equation (1) in the work by Zsiborács *et al*[89]. That study was based around a limited geographical area (Europe), which means that the same relationship for a theoretical global power grid like the one surveyed in this thesis could have significantly different results. Other studies, like the combined literature study by Cebulla *et al.*, observed similar exponential relationships between VRE penetration and energy storage capacity. However, apart from the exponential relationship, the actual values of capacity requirements observed by the authors had a high degree of variability, depending on many different factors. Because of this, the calculated ESS capacity in this thesis probably suffers from inaccuracies, especially compared to a real life, large scale deployment of VRE and ESS. It is also challenging to predict to what degree non-ESS factors, like demand response, improved forecasting, frequency response improvements and others will impact the requirements.

5.2 Technology Mix

Another important factor was the choice of technology mix. In this thesis, the total ESS capacity requirements were assumed to be covered by a constant 20 % battery share for all scenarios. Arguably, this is the most inaccurate part of the thesis, as a real life ESS technology mix would likely vary significantly between different technologies depending on a large number of different factors. The 20 % number was chosen based on the study by Alhelou *et al.*, which concentrated on the Spanish power grid and geography [5]. In that study, CAES was the dominant technology in terms of capacity, as it could provide long term, seasonal energy storage. It seems fair to assume that a real life, large scale transition to VRE and ESS would have a similar share of technologies, with the BESS being primarily used for short-term storage and other technologies, like TES, CAES or hydrogen being more suited to long term storage. This doesn't make battery storage any less useful, but it would allow a better allocation of the available resources if other, cheaper storage technologies are available for applications where batteries are less suited.

5.3 Raw Material Requirements and their Consequences

A consequence of the significant differences in required BESS capacity between the scenarios is large scenario-wise variations in raw material requirements. As lithium could be described as the most critical material in this analysis, it will be discussed first. Global lithium reserves were estimated by the USGS to be 21 million tonnes in 2021. The APS, which is the "medium ambition" scenario examined in this thesis, would require 1.595 million tonnes of lithium in total. If the global lithium reserve stayed constant, this requirement would account for 7.6 % of the global lithium reserve, which would be a substantial number. The STEPS scenario however, which is the least ambitious in this thesis, would require 779 000 tonnes, which is well within the current reserves. As the most ambitious scenario, NZE will require a total of 9.1 million tonnes of lithium until 2050. In this scenario, the lithium requirement of the global BESS industry would deplete 43 % of the global lithium reserve. This is a significantly more dramatic value than for the STEPS and APS scenarios.

While the NZE requirement is dramatic, there is reason to assume the global lithium reserve will increase, based on previous historical data and current identified lithium resources. In 2016, the global reserves were 16 million tonnes, significantly lower than the current figure of 21 million. Identified global lithium resources have recently increased and are currently at around 86 million tonnes. It is therefore likely that the future global reserves will increase, which could make the BESS lithium requirements of NZE less serious in an isolated context. However, even if reserves are expected to increase, the effects of the NZE scenario lithium requirements, combined with a dramatic increase in BEVs and other LIB-based electrification projects remains uncertain.

While the cumulative material requirements are relevant for the long term implications of each scenario, for the short- to mid term, the annual material demands are more important. Estimated 2021 lithium production (Excluding U.S. production due to protection of proprietary data) was 100 000 tonnes. NZE BESS lithium demand in 2032 is estimated to be 99 681 tonnes, according to the results estimated by BESSER. This illustrates that for the VRE and BESS deployment in the NZE scenario to be possible, a significant and rapid increase in annual lithium production is needed. For the APS scenario, annual lithium production of 100 000 tonnes isn't needed until 2047, but the 2030 values of over 29 000 tonnes will still be a significant challenge if current lithium production values are not increased rapidly. Even in the case of STEPS, the 2029 values of 24 800 tonnes is comparable to APS and could pose a challenge of similar magnitude.

Other potentially critical materials used in this analysis, like graphite and phosphate, could pose a challenge as well. The NZE scenario would need a cumulative 127 million tonnes of graphite by 2050. This is 40 % of the current global reserves, and the scenario would consume more graphite than the 2020 production levels of 1.1 million tonnes/year by 2032. However, unlike lithium, natural graphite has the advantage of having alternatives in synthetic graphite. The synthetic graphite production was 1.814 million tonnes in 2021, which was a larger figure than the natural graphite production. For the APS and STEPS scenarios, the graphite requirements are therefore less of an issue, but the short- and mid term requirements are still substantial, with an estimated 350 000 tonnes needed for the year 2032 in the STEPS scenario.

Unlike lithium and graphite, the NZE scenario's cumulative phosphate rock requirement of 92.62 million tonnes is only 0.12 % of the global reserves, and the 2050 demand of 7.26 million tonnes per year is well below 2020 production values of 223 million tonnes. However, phosphate rock is critical for world food security because of its use in fertilisers, with its use in fertiliser expected to reach

49 million tonnes in 2024. The world is expected to reach its maximum production of phosphorous ('Peak phosphorous') in a few decades, which could mean challenges to the global food security in the future[54]. It's therefore important to point out that the phosphorous requirement of the LFP batteries in this thesis may not significantly impact the global supply today, but the future of the global phosphate rock supply is uncertain, and should be reckoned with.

5.4 Greenhouse Gas Emissions

As with the other categories, the NZE scenario is by far the most emission intensive, with cumulative emissions of 8 billion tonnes CO_2Eq, as well as a 2050 annual emission rate of 582.4 million tonnes/year of CO_2Eq. To put these values into perspective, the 2017 CO_2 emissions of Canada were 573 million tonnes[22]. This is a significant emission rate, which illustrates that large-scale implementation of BESS will not come without a GHG emission cost. It is likely that the emission rate for LIB production will lower in the future as production processes switch to larger factories, use more renewable energy and use more efficient production methods for active materials, but it's difficult to predict exactly how "green" future battery production will become. The results of the GHG analysis also show that the emission rates of the APS and STEPS scenarios are significantly lower than for the NZE scenario. While these scenarios may result in lower total GHG emissions from their battery production (because they have a significantly lower BESS production rate), the NZE scenario still emits less GHG on a per-kWh basis, due to the higher share of renewable energy used in battery production.

To get the full picture, it's also critically important to consider what the BESS in this analysis are supposed to do: Replace much of the current fossil-fuelled electric power generation. According to the IEA, the 2019 global emissions from electricity and heat generation were 14 billion tonnes. In this context, NZE battery production emissions are 4.1 % of the annual emissions from electricity production today. Of course, a hypothetical NZE scenario would not only see large-scale deployment of BESS, but also the deployment of other types of ESS, as well as the installation of enough VRE sources to account for 68 % of global electricity production. The emissions from these systems also need to be taken into account to get a total picture of what the renewable energy transition will "cost" in terms of GHG emissions.

5.5 The Importance of Recycling

The results from this analysis highlight that a large-scale adoption of LIB BESS could bring with it high requirements in terms of battery production, raw material consumption and bring with it substantial greenhouse gas emissions. However, this analysis has not taken potential reuse and recycling into account. It is likely that the future LIB, automotive and ESS industry will transition to recycling programs in order to ease the demand for virgin materials and lower the environmental impact. According to Zeng *et al.*, it is critical for the industry to move towards large scale recovery and recycling programs as fast as possible[87].

In the context of this thesis, the NZE scenario is an outlier, by demanding by far the most BESS capacity and raw materials, and consequently emits significantly more GHG than APS and STEPS. An issue with NZE is therefore that it needs a large inflow of new batteries to satisfy the demand for BESS, especially in the decades after 2030. The corresponding outflow value doesn't match the

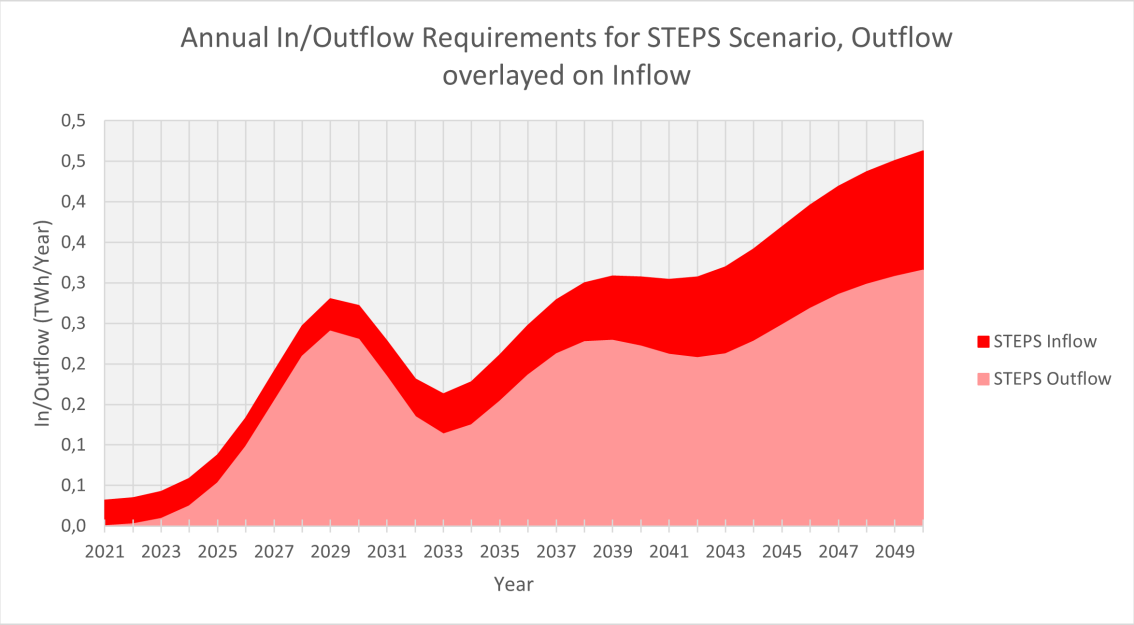

Figure 24: The inflow and overlaid outflow of battery capacity caused by LIB degradation for the STEPS Scenario.

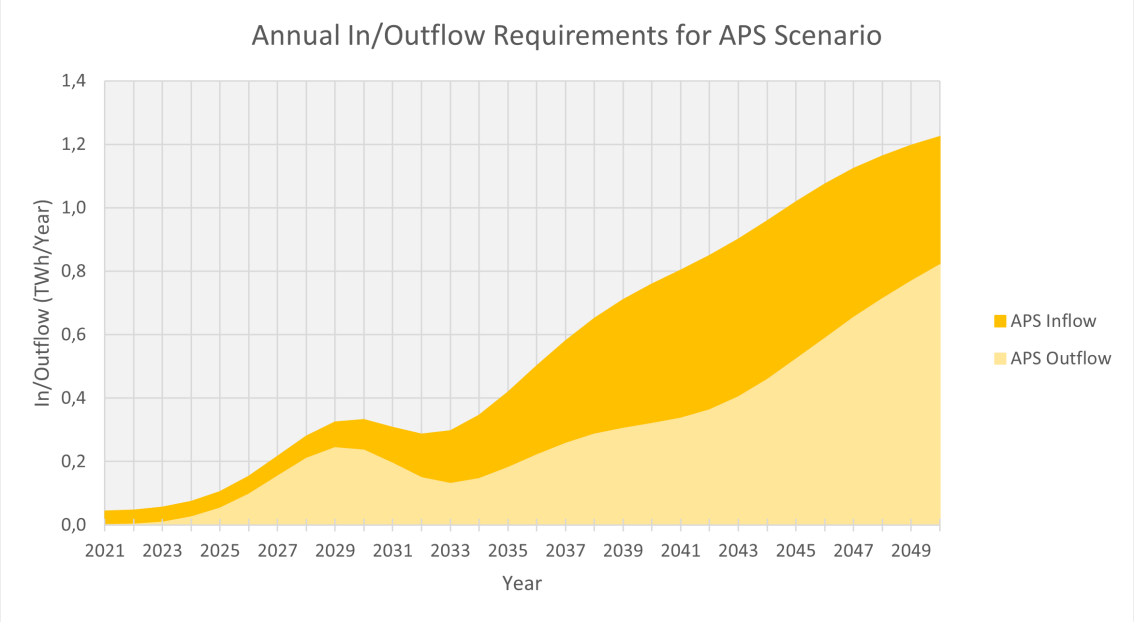

Figure 25: The inflow and overlaid outflow of battery capacity caused by LIB degradation for the APS Scenario.

inflow until later in the scenario. If the BESS industry is regarded as isolated in terms of recycling and recovery, then the recycled materials recovered from degraded BESS batteries will not be enough to cover the large increase in demand, even if 100 % recovery and recycling is assumed. Therefore, it is likely that the majority of the post-2030 inflow of NZE batteries would have to be covered by batteries manufactured with virgin materials.

With this in mind, the APS and STEPS scenarios both have better prerequisites to take advantage of recovery and recycling programs. Because the demand for new batteries in these scenarios increases more slowly, The in/outflow values are significantly closer to each other. Both of these

scenarios show a local maximum of both in and outflow in the late 2020s, which is mostly caused by the degradation of the BESS installations degrading and reaching their end of useful capacity, needing to be replaced. Figure 24 and 25 show the outflow rate overlaid on inflow rates of both the APS and STEPS scenarios. This demonstrates that it is possible to cover much of the needed battery inflow with recycled materials, assuming efficient, high yield recovery and recycling programs are rapidly implemented in the BESS industry.

5.6 Final Takeaways and Future Perspectives

This analysis has highlighted significant differences in BESS requirements from each of the three IEA scenarios. By using the equation from Zsiboraks *et al.* along with the VRE penetration and electricity demand values from the STEPS, APS and NZE scenarios, it was found that NZE would require significantly more installed BESS capacity than the other scenarios, mostly as a result of the close to exponential relationship between VRE penetration and energy storage fraction. This difference would propagate itself to the other requirements, with the NZE scenario dominating the other scenarios in both in- and outflow, raw material requirements and greenhouse gas emissions. However, there are significant uncertainties regarding the accuracy of the original BESS capacity and technology mix estimates, as they are based on models concentrating on specific geographic areas, as no global model for ESS capacity and VRE penetration could be obtained.

With this said, the APS and STEPS scenarios would also require a large amount of raw materials and battery manufacturing capability within 8 years from today, if the required installed BESS capacity is to be satisfied. The greenhouse gas emissions of all three scenarios are also significant on their own, with the NZE scenario being especially intensive in this regard. While large-scale recycling programs can and should be implemented to limit the raw material requirements and environmental impacts of all three scenarios, the effect of recycling is limited in the 'ramp-up' period of the NZE scenario due to the high capacity inflow needed from the 2030's. However, recycling would be able to cover much of the needed capacity inflows in the APS and STEPS scenarios, due to their lower requirement in regards to inflow.

An important factor to consider is that the BESS requirements highlighted in this thesis do not exist in a vacuum. The LIB industry is currently producing batteries for personal electronics, a rapidly growing BEV market and the burgeoning BESS market. Both the BEV and BESS are predicted to grow rapidly in the coming decades. For the results of this thesis to be properly evaluated, they will need to be viewed in a symbiotic relationship with the rest of the LIB industry and global production networks, so that proper strategies for the battery and ESS industry can be developed, both for the long- and short-term time frames. Additionally, more research and investment in ESS-specific battery technology and alternative, non-battery methods of energy storage is needed. The results of this analysis show that current LFP-based LIB technology is suitable for ESS applications. However, it is still a technology that requires significant amounts of resource- and energy intensive raw materials, especially as the high energy density of the lithium ion battery may not strictly be needed in stationary ESS applications if cheaper and less resource-intensive options are available. If future LIB resource availability becomes more challenging, it is likely that more of the available LIB resources would be allocated for applications where the advantages of LIBs are needed and no alternatives exist, for example in the transportation sector.

6 Conclusion

The goal of this thesis was to forecast the requirements of global deployment of lithium ion battery energy storage systems (LIB ESS), based on an increase in variable renewable energy (VRE) penetration in the global power grid. The analysis was based on three scenarios from the International Energy Agency: The Stated Policies Scenario (STEPS), Announced Pledges Scenario (APS) and Net Zero by 2050 Scenario (NZE). The following requirements were estimated for each scenario:

A. The required global installed LIB ESS capacity.

B. The inflow and outflow of LIB ESS to sustain the required installed capacity.

C. The raw material required to sustain the estimated inflow and outflow values.

D. The greenhouse gas emissions of manufacturing the required amount of LIB ESS systems.

By developing a spreadsheet model, the Battery Energy Storage System Estimated Requirement Model (BESSER), all four requirements were analysed for each scenario. The analysis showed that the requirements of the NZE scenario was the highest in all four categories, followed by APS and STEPS. NZE would require 18 times as much installed LIB BESS capacity than STEPS, and 6.5 times as much as APS. When taking into account the in-and outflow of LIB ESS due to degradation, the cumulative battery requirement of the NZE, APS and STEPS scenarios were 102.13, 17.97 and 8.78 TWh respectively. To satisfy these inflow requirements, cumulative a lithium requirement of 9.06 million, 1.6 million and 779 000 tonnes were needed for NZE, APS and STEPS. Annual greenhouse gas emissions for each scenario in 2050 were 582 million, 103 million and 42 million tonnes of CO_2Eq.

In the analysis, it was found that the VRE penetration value had a large influence on the required capacity of energy storage, which was the primary reason for the significant requirements of the NZE scenario. All scenarios would require an increased inflow of battery capacity at the end of the 2020's to replace degraded systems. The raw material requirement for NZE was found to be very large, with the cumulative lithium requirement of the scenario being 43 % of current reserves, as well as exceeding 2021 global lithium production figures by 2032. The APS and STEPS scenarios had significantly raw material requirements and greenhouse gas emissions. Great potential for recycling was observed, especially in APS and STEPS. In NZE, recycling would have limited value in the initial ramp up period, but would still be of importance later in the scenario when in/outflow values stabilised.

Transitioning global electricity production away from fossil fuels will not come without its challenges. When more variable renewable energy is deployed, the need for reliable and efficient energy storage increases too. With lithium ion batteries likely to be part of the future ESS solution, the results discussed in this thesis show that global deployment of lithium ion ESS may require significant investments in manufacturing facilities, mining and recycling programs. Additionally, these requirements must be viewed in context with the wider LIB market in order to properly assess the consequences of LIB BESS adoption.

6.1 Further Work

In order to get a better picture of global ESS capacity requirements, more accurate modelling of VRE deployment and its effect on the power grid is needed. Future work should examine the power requirement of ESS as well, which was not done in this thesis. Additionally, a higher variety of battery technologies, including more exotic types like lithium sulphur and flow batteries, should probably be assumed to be part of the future BESS mix.

7 Appendix

The BESSER spreadsheet created for this thesis is available as the attatched file ”Attachment1.xlsx”

7.1 VRE penetration in NZE, APS and STEPS

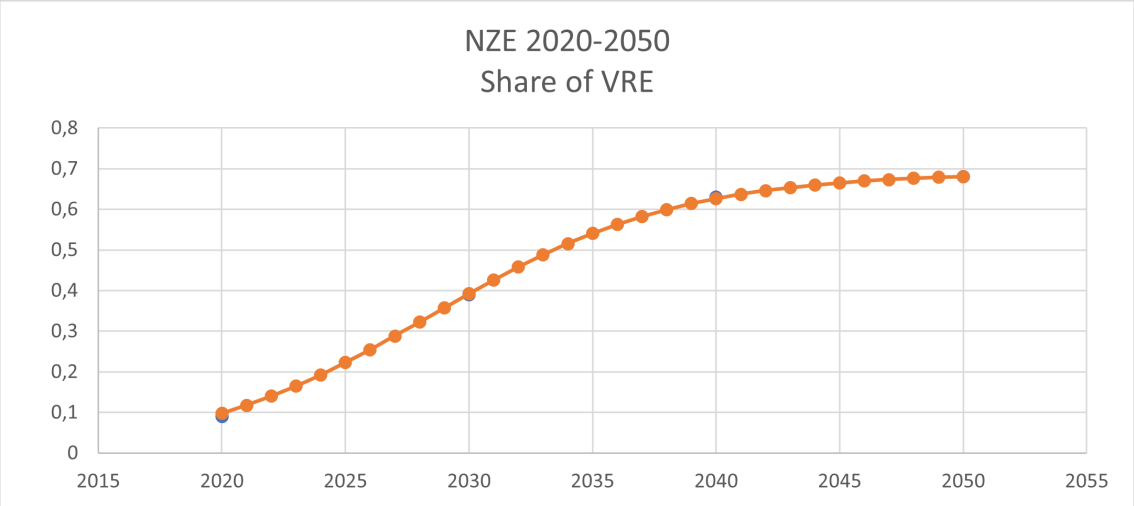

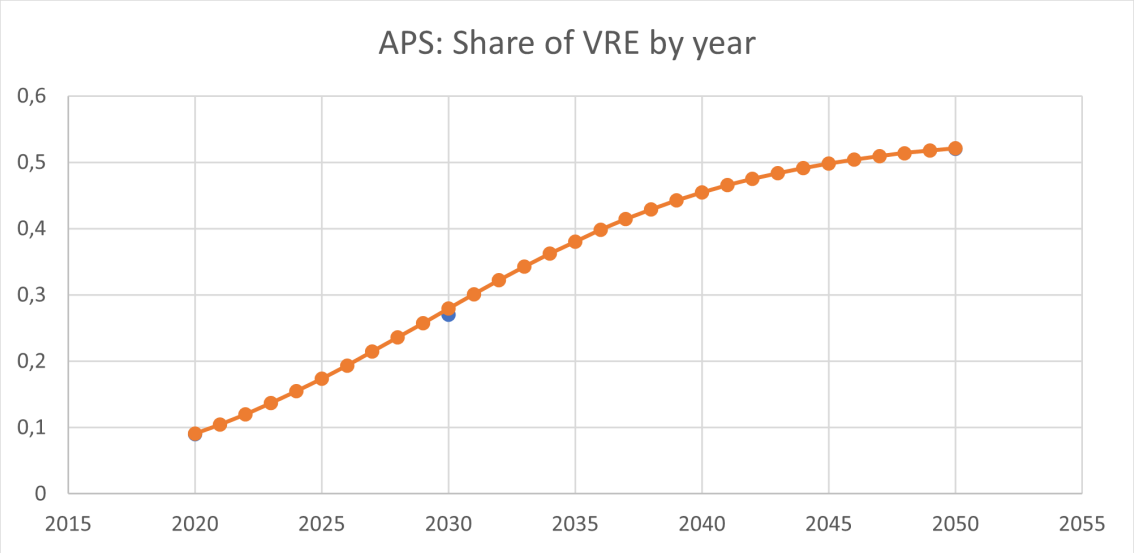

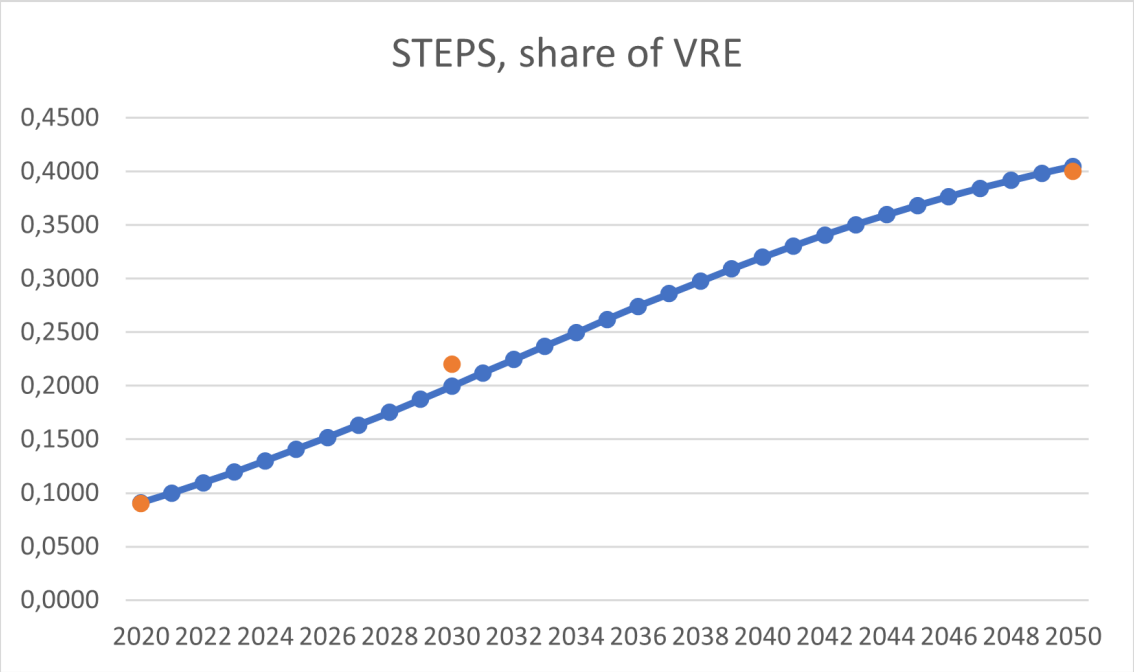
STEPS, share of VRE
0,4500
0,4000
0,3500
0,3000
0,2500
0,2000
0,1500
0,1000
0,0500
0,0000
2020 2022 2024 2026 2028 2030 2032 2034 2036 2038 2040 2042 2044 2046 2048 2050

Bibliography

[1] Sara Abada et al. 'Combined experimental and modeling approaches of the thermal runaway of fresh and aged lithium-ion batteries'. In: *Journal of Power Sources* 399 (2018), pp. 264–273.

[2] Victor Agubra and Jeffrey Fergus. 'Lithium ion battery anode aging mechanisms'. In: *Materials* 6.4 (2013), pp. 1310–1325.

[3] Shabbir Ahmed, Paul A Nelson and Dennis W Dees. 'Study of a dry room in a battery manufacturing plant using a process model'. In: *Journal of Power Sources* 326 (2016), pp. 490–497.

[4] *Air could be the world's next battery.* 2017. URL: https://www.sintef.no/en/latest-news/2017/air-could-be-the-worlds-next-battery/ (visited on 21st June 2022).

[5] Hassan Haes Alhelou et al. 'Assessing the optimal generation technology mix determination considering demand response and EVs'. In: *International Journal of Electrical Power & Energy Systems* 119 (2020), p. 105871.

[6] Guruprasad Alva, Yaxue Lin and Guiyin Fang. 'An overview of thermal energy storage systems'. In: *Energy* 144 (2018), pp. 341–378.

[7] *Announced Pledges Scenario (APS).* 2021. URL: https://www.iea.org/reports/world-energy-model/announced-pledges-scenario-aps (visited on 24th June 2022).

[8] *Base Load Energy Sustainability.* URL: https://www.e-education.psu.edu/eme807/node/667 (visited on 24th June 2022).

[9] *BatPaC V2 Beta.* URL: https://www.epa.gov/sites/default/files/2016-11/bat-pa-c-v2-beta.xlsx (visited on 24th June 2022).

[10] Jürgen O Besenhard. *Handbook of battery materials.* John Wiley & Sons, 2008.

[11] Lori Bird, Michael Milligan and Debra Lew. *Integrating variable renewable energy: Challenges and solutions.* Tech. rep. National Renewable Energy Lab.(NREL), Golden, CO (United States), 2013.

[12] *BMW Is Turning Used i3 Batteries Into Home Energy Storage Units.* URL: https://fuelsaveglobal.com/bmw-is-turning-used-i3-batteries-into-home-energy-storage-units/ (visited on 24th June 2022).

[13] Silvia Bobba, Fabrice Mathieux and Gian Andrea Blengini. 'How will second-use of batteries affect stocks and flows in the EU? A model for traction Li-ion batteries'. In: *Resources, Conservation and Recycling* 145 (2019), pp. 279–291.

[14] Lisa Bongartz et al. 'Multidimensional criticality assessment of metal requirements for lithium-ion batteries in electric vehicles and stationary storage applications in Germany by 2050'. In: *Journal of Cleaner Production* 292 (2021), p. 126056.

[15] Stéphanie Bouckaert et al. 'Net Zero by 2050: A Roadmap for the Global Energy Sector'. In: (2021).

[16] Martin Brand et al. 'Electrical safety of commercial Li-ion cells based on NMC and NCA technology compared to LFP technology'. In: *World Electric Vehicle Journal* 6.3 (2013), pp. 572–580.

[17] Silje Nornes Bryntesen et al. 'Opportunities for the State-of-the-Art Production of LIB Electrodes—A Review'. In: *Energies* 14.5 (2021), p. 1406.

[18] Isidor Buchmann. 'Batteries in a portable world: a handbook on rechargeable batteries for non-engineers, 4th edition'. In: (2017).

[19] Odne Stokke Burheim. *Engineering energy storage*. Academic press, 2017.

[20] *Carbon Dioxide Emissions From Electricity*. 2021. URL: https://www.world-nuclear.org/information-library/energy-and-the-environment/carbon-dioxide-emissions-from-electricity.aspx (visited on 23rd June 2022).

[21] Felix Cebulla et al. 'How much electrical energy storage do we need? A synthesis for the US, Europe, and Germany'. In: *Journal of Cleaner Production* 181 (2018), pp. 449–459.

[22] *CO2 Emissions*. URL: https://ourworldindata.org/co2-emissions (visited on 24th June 2022).

[23] Andy Colthorpe. *Investigation confirms cause of fire at Tesla's Victorian Big Battery in Australia*. 2022. URL: https://www.energy-storage.news/investigation-confirms-cause-of-fire-at-teslas-victorian-big-battery-in-australia/ (visited on 20th June 2022).

[24] Qiang Dai et al. 'Life cycle analysis of lithium-ion batteries for automotive applications'. In: *Batteries* 5.2 (2019), p. 48.

[25] Paul Denholm et al. *Inertia and the power grid: A guide without the spin*. Tech. rep. National Renewable Energy Lab.(NREL), Golden, CO (United States), 2020.

[26] Jan Diekmann and Arno Kwade. *Recycling of lithium-ion batteries: The LithoRec Way*. Springer, 2018.

[27] Yuanli Ding et al. 'Automotive Li-ion batteries: current status and future perspectives'. In: *Electrochemical Energy Reviews* 2.1 (2019), pp. 1–28.

[28] Simon Duehnen et al. 'Toward green battery cells: perspective on materials and technologies'. In: *Small Methods* 4.7 (2020), p. 2000039.

[29] *Electricity explained: How electricity is delivered to consumers*. 2021. URL: https://www.eia.gov/energyexplained/electricity/delivery-to-consumers.php (visited on 24th June 2022).

[30] *Electricity Production and Distribution*. 2020. URL: https://afdc.energy.gov/fuels/electricity_production.html (visited on 24th June 2022).

[31] Linda Ager-Wick Ellingsen, Christine Roxanne Hung and Anders Hammer Strømman. 'Identifying key assumptions and differences in life cycle assessment studies of lithium-ion traction batteries with focus on greenhouse gas emissions'. In: *Transportation Research Part D: Transport and Environment* 55 (2017), pp. 82–90.

[32] Erik Emilsson and Lisbeth Dahllöf. 'Lithium-ion vehicle battery production'. In: *IVL Swedish Environmental Research Institute: Stockholm, Sweden* (2019).

[33] Xuning Feng et al. 'Thermal runaway mechanism of lithium ion battery for electric vehicles: A review'. In: *Energy Storage Materials* 10 (2018), pp. 246–267.

[34] Jan Figgener et al. 'The development of stationary battery storage systems in Germany–A market review'. In: *Journal of energy storage* 29 (2020), p. 101153.

[35] Federica Forte et al. 'Lithium iron phosphate batteries recycling: An assessment of current status'. In: *Critical Reviews in Environmental Science and Technology* 51.19 (2021), pp. 2232–2259.

[36] Xinkai Fu et al. 'Perspectives on cobalt supply through 2030 in the face of changing demand'. In: *Environmental science & technology* 54.5 (2020), pp. 2985–2993.

[37] Max Roser Hannah Ritchie. *Electricity Mix*. 2022. URL: https://ourworldindata.org/electricity-mix (visited on 23rd June 2022).

[38] Han Hao et al. 'GHG Emissions from the production of lithium-ion batteries for electric vehicles in China'. In: *Sustainability* 9.4 (2017), p. 504.

[39] Gavin Harper et al. 'Recycling lithium-ion batteries from electric vehicles'. In: *nature* 575.7781 (2019), pp. 75–86.

[40] Heiner Hans Heimes et al. *Lithium-ion battery cell production process*. PEM der RWTH Aachen University, 2018.

[41] Veronika Henze. *Battery Pack Prices Fall to an Average of dollar 132/KWh, But Rising Commodity Prices Start to Bite*. 2021.

[42] *History of Power: The Evolution of the Electric Generation Industry*. 2020. URL: https://www.powermag.com/history-of-power-the-evolution-of-the-electric-generation-industry/ (visited on 23rd June 2022).

[43] *How can electricity be stored with batteries?* 2021. URL: https://totalenergies.com/infographics/how-can-electricity-be-stored-batteries (visited on 20th June 2022).

[44] Imad Idelah. *Li-ion Cell Types*. URL: https://news.inventuspower.com/blog/li-ion-cell-types. (accessed: 15.12.2021).

[45] IEA. *Energy Storage*. URL: https://www.iea.org/reports/energy-storage. (accessed: 2.6.2022).

[46] Clean Energy Institute. *What are some advantages of Li-ion batteries?* URL: https://www.cei.washington.edu/education/science-of-solar/battery-technology/. (accessed: 15.12.2021).

[47] *Is the Juice Worth the Squeeze? Compressed Air Energy Storage for Grid-Scale Power*. 2021. URL: https://schaperintl.com/is-the-juice-worth-the-squeeze-compressed-air-energy-storage-for-grid-scale-power/ (visited on 21st June 2022).

[48] Christian M Julien, Xiaoyu Zhang and Alain Mauger. 'Lithium Iron Phosphate: Olivine Material for High Power Li-Ion Batteries'. In: *Res Dev Mater Sci* 2 (2017), pp. 3–6.

[49] Rennie B Kaunda. 'Potential environmental impacts of lithium mining'. In: *Journal of Energy & Natural Resources Law* 38.3 (2020), pp. 237–244.

[50] Peter Keil et al. 'Calendar aging of lithium-ion batteries'. In: *Journal of The Electrochemical Society* 163.9 (2016), A1872.

[51] Ånund Killingtveit. 'Hydroelectric power'. In: *Future Energy*. Elsevier, 2014, pp. 453–470.

[52] M Kostic. 'Work, power, and energy'. In: (2004).

[53] Peter Kurzweil. 'lithium battery energy storage: State of the art including lithium–air and lithium–sulfur systems'. In: *Electrochemical energy storage for renewable sources and grid balancing* (2015), pp. 269–307.

[54] Binlin Li, Kathryn B Bicknell and Alan Renwick. 'Peak phosphorus, demand trends and implications for the sustainable management of phosphorus in China'. In: *Resources, Conservation and Recycling* 146 (2019), pp. 316–328.

[55] Rebecca Lindsey. *Climate Change: Atmospheric Carbon Dioxide*. 2022. URL: https://www.climate.gov/news-features/understanding-climate/climate-change-atmospheric-carbon-dioxide (visited on 23rd June 2022).

[56] Francesco Lo Franco et al. 'Efficiency Comparison of DC and AC Coupling Solutions for Large-Scale PV+ BESS Power Plants'. In: *Energies* 14.16 (2021), p. 4823.

[57] Pure Energy Minerals. *Where did that lithium come from?* 2022. URL: https://pureenergyminerals.com/technology-overview/ (visited on 4th June 2022).

[58] Gavin M Mudd. 'Global trends and environmental issues in nickel mining: Sulfides versus laterites'. In: *Ore Geology Reviews* 38.1-2 (2010), pp. 9–26.

[59] Bernard Muhon. 'Stocker l'électricité: Oui, c'est indispensable, et c'est possible! pourquoi, où, comment'. In: *Paris, France: ECRIN* (2003).

[60] Akshaya K Padhi, Kirakodu S Nanjundaswamy and John B Goodenough. 'Phospho-olivines as positive-electrode materials for rechargeable lithium batteries'. In: *Journal of the electrochemical society* 144.4 (1997), p. 1188.

[61] CD Parker. 'APPLICATIONS–STATIONARY— Energy storage systems: batteries'. In: (2009).

[62] Gaetan Patry et al. 'Cost modeling of lithium-ion battery cells for automotive applications'. In: *Energy Science & Engineering* 3.1 (2015), pp. 71–82.

[63] Claudia Pavarini. 'Battery storage is (almost) ready to play the flexibility game'. In: (2019).

[64] Melissa Pistilli. *Top 9 Nickel-producing Countries (Updated 2022)*. 2022. URL: https://investingnews.com/daily/resource-investing/base-metals-investing/nickel-investing/top-nickel-producing-countries/ (visited on 4th June 2022).

[65] Yuliya Preger et al. 'Degradation of commercial lithium-ion cells as a function of chemistry and cycling conditions'. In: *Journal of The Electrochemical Society* 167.12 (2020), p. 120532.

[66] Ghanim Putrus and Edward Bentley. 'Integration of distributed renewable energy systems into the smart grid'. In: *Electric Renewable Energy Systems* (2016), pp. 487–518.

[67] Gilpin R Robinson Jr, Jane M Hammarstrom and Donald W Olson. *Graphite*. Tech. rep. US Geological Survey, 2017.

[68] Michael Roscher. *Zustandserkennung von lifepo4-batterien für Hybrid-und Elektrofahrzeuge*. Shaker, 2011.

[69] John F Slack, Bryn E Kimball and Kim B Shedd. *Cobalt*. Tech. rep. US Geological Survey, 2017.

[70] M Sonoda et al. 'Development of containerized energy storage system with lithium-ion batteries'. In: *Mitsubishi Heavy Industries Technical Review* 50.3 (2013), p. 36.

[71] Lena Spitthoff, Paul R Shearing and Odne Stokke Burheim. 'Temperature, Ageing and Thermal Management of Lithium-Ion Batteries'. In: *Energies* 14.5 (2021), p. 1248.

[72] R Spotnitz and J Franklin. 'Abuse behavior of high-power, lithium-ion cells'. In: *Journal of power sources* 113.1 (2003), pp. 81–100.

[73] *Stated Policies Scenario (STEPS)*. 2021. URL: https://www.iea.org/reports/world-energy-model/stated-policies-scenario-steps#abstract (visited on 24th June 2022).

[74] Florian Steinke, Philipp Wolfrum and Clemens Hoffmann. 'Grid vs. storage in a 100% renewable Europe'. In: *Renewable Energy* 50 (2013), pp. 826–832.

[75] Wood Mackenzie Energy Storage. *Supply Chain Looms as Serious Threat to Batteries' Green Reputation*. 2019. URL: https://www.greentechmedia.com/articles/read/graphite-the-biggest-threat-to-batteries-green-reputation (visited on 4th June 2022).

[76] Mohammed Yekini Suberu, Mohd Wazir Mustafa and Nouruddeen Bashir. 'Energy storage systems for renewable energy power sector integration and mitigation of intermittency'. In: *Renewable and Sustainable Energy Reviews* 35 (2014), pp. 499–514.

[77] Mineral Commodity Summaries et al. 'Mineral commodity summaries'. In: *US Geological Survey: Reston, VA, USA* 200 (2021).

[78] *The Composition of EV Batteries: Cells? Modules? Packs? Let's Understand Properly!* 2022. URL: https://www.samsungsdi.com/column/all/detail/54344.html (visited on 20th June 2022).

[79] Ozan Toprakci et al. 'Fabrication and electrochemical characteristics of LiFePO4 powders for lithium-ion batteries'. In: *KONA Powder and Particle Journal* 28 (2010), pp. 50–73.

[80] Emmanuel Umpula, Abbi Buxton and Brendan Schwartz. 'Islands of responsibility?' In: *Natural resource management* (2021).

[81] *Vekselstrøm (AC current)*. 2020. URL: https://snl.no/vekselstr%5C%C3%5C%B8m (visited on 24th June 2022).

[82] Q. Wang. 'Comparative Analysis of Cathode Materials Based on Life Cycle Assessment'. In: *Transportation Research Part D: Transport and Environment* (2012).

[83] Johannes Weniger, Tjarko Tjaden and Volker Quaschning. 'Sizing of residential PV battery systems'. In: *Energy Procedia* 46 (2014), pp. 78–87.

[84] David L Wood III, Jianlin Li and Claus Daniel. 'Prospects for reducing the processing cost of lithium ion batteries'. In: *Journal of Power Sources* 275 (2015), pp. 234–242.

[85] Rui Xiong et al. 'Lithium-ion battery aging mechanisms and diagnosis method for automotive applications: Recent advances and perspectives'. In: *Renewable and Sustainable Energy Reviews* 131 (2020), p. 110048.

[86] Rui Xiong et al. 'Toward a safer battery management system: A critical review on diagnosis and prognosis of battery short circuit'. In: *Iscience* 23.4 (2020), p. 101010.

[87] Xianlai Zeng, Jinhui Li and Narendra Singh. 'Recycling of spent lithium-ion battery: a critical review'. In: *Critical Reviews in Environmental Science and Technology* 44.10 (2014), pp. 1129–1165.

[88] Jun-chao Zheng et al. 'LiFePO4 with enhanced performance synthesized by a novel synthetic route'. In: *Journal of Power Sources* 184.2 (2008), pp. 574–577.

[89] Henrik Zsiborács et al. 'Intermittent renewable energy sources: The role of energy storage in the european power system of 2040'. In: *Electronics* 8.7 (2019), p. 729.

[90] Ghassan Zubi et al. 'The lithium-ion battery: State of the art and future perspectives'. In: *Renewable and Sustainable Energy Reviews* 89 (2018), pp. 292–308.

NTNU

Norwegian University of
Science and Technology